In-beam performance of a Resistive Plate Chamber operated with eco-friendly gas mixtures

L. Quaglia[a], on behalf of the ALICE and RPC ECOgas@GIF++ collaborations. **The RPC ECOgas@GIF++ collaboration:** M. Abbrescia[f,c], G. Aielli[u], R. Aly[c,h], M. C. Arena[q], M. Barroso[k], L. Benussi[d], S. Bianco[d], D. Boscherini[g], F. Bordon[p], A. Bruni[g], S. Buontempo[r], M. Busato[p], P. Camarri[u], R. Cardarelli[m], L. Congedo[c], D. De Jesus Damiao[k], M. De Serio[f,c], A. Di Ciaccio[u], L. Di Stante[u], P. Dupieux[n], J. Eysermans[s], A. Ferretti[l,a], G. Galati[f,c], M. Gagliardi[l,a], R. Guida[p], G. Iaselli[b,c], B. Joly[n], S.A. Juks[x], K.S. Lee[w], B. Liberti[m], D. Lucero Ramirez[v], B. Mandelli[p], S.P. Manen[n], L. Massa[g], A. Pastore[c], E. Pastori[m], D. Piccolo[d], L. Pizzimento[m], A. Polini[g], G. Proto[m], G. Pugliese[b,c], D. Ramos[b,c], G. Rigoletti[p], A. Rocchi[m], M. Romano[g], A. Samalan[j], P. Salvini[i], R. Santonico[u], G. Saviano[e], M. Sessa[m], S. Simone[f,c], L. Terlizzi[l,a], M. Tytgat[j,t], E. Vercellin[l,a], M. Verzeroli[o], N. Zaganidis[v]

[a] *INFN Sezione di Torino, Via P. Giuria 1, Torino, 10125, Italy,*
[b] *Politecnico di Bari, Dipartimento Interateneo di Fisica, via Amendola 173, Bari, 70125, Italy,*
[c] *INFN Sezione di Bari, Via E. Orabona 4, Bari, 70125, Italy,*
[d] *INFN - Laboratori Nazionali di Frascati, Via Enrico Fermi 54, Frascati (Roma), 00044, Italy,*
[e] *Sapienza Università di Roma, Dipartimento di Ingegneria Chimica Materiali Ambiente, Piazzale Aldo Moro 5, Roma, 00185, Italy,*
[f] *Università degli studi di Bari, Dipartimento Interateneo di Fisica, Via Amendola 173, Bari, 70125, Italy,*
[g] *INFN Sezione di Bologna, Via C. Berti Pichat 4/2, Bologna, 40127, Italy,*
[h] *Helwan University, , Helwan, Cairo Governorate, 4037120, Egypt,*
[i] *INFN Sezione di Pavia, Via A. Bassi 6, Pavia, 27100, Italy,*
[j] *Ghent University, Dept. of Physics and Astronomy, Proeftuinstraat 86, Ghent, B-9000, Belgium,*
[k] *Universidade do Estado do Rio de Janeiro, R. São Francisco Xavier, 524, Maracanã, Rio de Janeiro - RJ, 20550-013, Brazil,*
[l] *Università degli studi di Torino, Dipartimento di Fisica, Via P. Giuria 1, Torino, 10125, Italy,*
[m] *INFN Sezione di Roma Tor Vergata, Via della Ricerca Scientifica 1, Roma, 00133, Italy,*
[n] *Clermont Université, Université Blaise Pascal, CNRS/IN2P3, Laboratoire de Physique Corpusculaire, BP 10448, Clermont-Ferrand, F-63000, France,*
[o] *Universitè Claude Bernard Lyon I, 43 Bd du 11 Novembre 1918, Villeurbanne, 69100, France,*
[p] *CERN, Espl. des Particules 1, Meyrin, 1211, Switzerland,*
[q] *Università degli studi di Pavia, Corso Strada Nuova 65, Pavia, 27100, Italy,*
[r] *INFN Sezione di Napoli, Complesso universitario di Monte S. Angelo ed. 6 Via Cintia, Napoli, 80126, Italy,*
[s] *Massachusetts Institute of Technology, 77 Massachusetts Ave, Cambridge, MA, 02139, USA,*
[t] *Vrije Universiteit Brussel (VUB-ELEM), Dept. of Physics, Pleinlaan 2, Brussels, 1050, Belgium,*
[u] *Università degli studi di Roma Tor Vergata, Dipartimento di Fisica, Via della Ricerca Scientifica 1, Roma, 00133, Italy,*
[v] *Universidad Iberoamericana, Dept. de Fisica y Matematicas, , Mexico City, 01210, Mexico,*
[w] *Korea University, 145 Anam-ro, Seongbuk-gu, Seoul, , Korea,*
[x] *Université Paris-Saclay, 3 rue Joliot Curie, Bâtiment Breguet, Gif-sur-Yvette, 91190, France,*

Abstract

ALICE (A Large Ion Collider Experiment) studies the Quark-Gluon Plasma (QGP): a deconfined state of nuclear matter obtained in ultra-relativistic heavy-ion collisions. One of the key probes for QGP characterization is the study of quarkonia and open heavy flavour production, of which ALICE exploits the muonic decay. In particular, a set of Resistive Plate Chambers (RPCs), placed in the forward rapidity region of the ALICE detector, is used for muon identification purposes.

The correct operation of these detectors is ensured by the choice of the proper gas mixture. Currently they are operated with a mixture of $C_2H_2F_4$, i-C_4H_{10} and SF_6 but, starting from 2017, new EU regulations have enforced a progressive phase-out of $C_2H_2F_4$ because of its large Global Warming Potential (GWP), which is making it difficult and costly to purchase. Moreover, CERN asked LHC experiments to reduce greenhouse gases emissions, to which RPC operation contributes significantly.

A possible candidate for $C_2H_2F_4$ replacement is the $C_3H_2F_4$ (diluted with other gases, such as CO_2), which has been extensively tested using cosmic muons. Promising gas mixtures have been devised; the next crucial steps are the detailed in-beam characterization of such mixtures as well as the study of their performance under increasing irradiation levels.

This contribution will describe the methodology and results of beam tests carried out at the CERN Gamma Irradiation Facility (equipped with a high activity ^{137}Cs source and muon beam) with an ALICE-like RPC prototype, operated with several mixtures with varying proportions of CO_2, $C_3H_2F_4$, i-C_4H_{10} and SF_6 . Absorbed currents, efficiencies, prompt charges, cluster sizes, time resolutions and rate capabilities will be presented, both from digitized (for detailed shape and charge analysis) and discriminated (using the same front-end electronics as employed in ALICE) signals.

Keywords: Resistive Plate Chambers, Beam test, Eco-friendly gas mixtures

A miniaturized magnetic field sensor based on nitrogen-vacancy centers

Stefan Dix,[1,*] Dennis Lönard,[1,*] Isabel Cardoso Barbosa,[1] Jonas Gutsche,[1] Jonas Witzenrath,[1] and Artur Widera[1,†]

[1] *Department of Physics and State Research Center OPTIMAS, University of Kaiserslautern, Erwin-Schroedinger-Str. 46, 67663 Kaiserslautern, Germany*

(Dated: March 1, 2024)

The nitrogen-vacancy (NV) center in diamond is a prime candidate for quantum sensing technologies. Ongoing miniaturization calls for ever-smaller sensors maintaining good measurement performance. Here, we present a fully integrated mechanically robust fiber-based endoscopic sensor capable of $5.9\,\mathrm{nT}/\sqrt{\mathrm{Hz}}$ magnetic field sensitivity utilizing 15 µm sized microdiamonds at a microwave power of 50 mW and optical power of 2.15 mW. A direct laser writing process is used to localize a diamond containing NV centers above the fiber's core by a polymer structure. This structure enables stable optical access and independent guiding of excitation and fluorescent light in different optical fibers. This separation strongly reduces the contribution of autofluorescence from the excitation light in the optical fiber. Moreover, a metallic direct laser written antenna structure is created next to the fibers' facet, allowing microwave manipulation of the NV centers' spins. The fabricated endoscopic sensor provides a robust platform with a tip diameter of 1.25 mm. The device enables remote optical and microwave access to perform the full range of coherent spin measurements with NV centers at a spatial resolution of 15 µm. We demonstrate the capability of vector magnetic field measurements in a magnetic field as used in state-of-the-art ultracold quantum gas experiments, opening a potential field in which high resolution and high sensitivity are necessary.

I. INTRODUCTION

The negatively charged nitrogen-vacancy (NV) center in diamond is an atomic-scale point defect in the diamond lattice consisting of a vacancy and a substitutional nitrogen atom next to it [1, 2]. It provides optically addressable spin states and allows optical readout of the spin-state population [3]. When resonantly excited with a microwave (MW) field, it enables, due to spin-dependent intersystem crossing, optically detected magnetic resonance (ODMR) spectroscopy [4]. The inclusion of the defect in the diamond lattice results in a solid-state sensor with atom-like behavior [5], making it a leading candidate in research as a highly sensitive vectorial magnetic field sensor with high spatial resolution [6] and the capability to measure temperature [7, 8], pressure [9], and electrical fields [10–13]. Other magnetic-field sensors such as superconducting quantum interference devices (SQUIDs) and optically pumped atomic magnetometers (OPAMs) have demonstrated sensitivities in the $\mathrm{fT}/\sqrt{\mathrm{Hz}}$ range [14, 15]. However, they often require cryogenic temperatures or are not intrinsically capable of measuring vectorial magnetic fields with a single sensing element. Many applications, like measurements of electrical currents in coils or high-power electronics, paramagnetic materials, or permanent magnetic materials, need to be measured accurately with $\mathrm{nT}/\sqrt{\mathrm{Hz}}$ sensitivities [16–19]. Often, they require only moderate absolute sensitivities, but strongly profit from an increased sensitivity per distance [20–22] or if high sensitivity is necessary can be achieved by increasing the number of spins and volume [23, 24]. Here, diamonds containing NV centers provide high overall sensitivities and the usability from cryogenic temperatures up to hundreds of °C [25–27] promising to be the next generation of magnetic field sensors.

Moreover, single diamond-based sensors have demonstrated vector magnetometry with a wide dynamic range and high sensitivity [16]. Current state-of-the-art approaches to measuring magnetic fields are based on stationary setups such as wide-field microscopy utilizing diamond plates [28], scanning diamond probes [29], or integrated portable devices [30]. The reported portable devices can be split up into two groups. Either they are fully integrated, consisting of necessary excitation and detection elements such as MW antennas, optical excitation light sources, and detectors close by or directly attached [31–33]. Alternatively, they consist of two parts where the sensor's head, as well as the excitation and detection sections, are separated with optical fibers and electrical wires [34–38]. However, integrating these elements, such as detectors and excitation sources, limits the possible miniaturization of the actual sensor. Therefore, miniaturization can be enhanced by only integrating the necessary elements on a sensor's tip and connecting them to wires and optical fibers. Combining an NV-doped diamond with optical and microwave access on a compact form factor leads to challenges in finding a robust platform. Previously reported results suggest that positioning the microwave emitting element near the diamond can provide a good sensitivity even at low power settings [39].

In this context, an important limitation of miniaturized optical fiber-based sensors is the so-called autofluorescence of optical fibers [40, 41]. This fluorescence arises from the necessary excitation light required for NV centers, which excites photo-active

* Both authors contributed equally
† widera@physik.uni-kl.de

QRIS: A Quantitative Reflectance Imaging System for the Pristine Sample of Asteroid Bennu

Ruby E. Fulford[1], Dathon R Golish[1], Dante S. Lauretta[1], Daniella N. DellaGiustina[1], Steve Meyer[1], Nicole Lunning[2], Christopher Snead[2], Jason P. Dworkin[3], Carina A. Bennett[1], Harold C. Connolly, Jr.[1,4,5], Taylor Johnson[6], Anjani T. Polit[1], Pierre Haenecour[1], and Andrew J. Ryan[1]

[1]Lunar and Planetary Laboratory, University of Arizona, Tucson, AZ, USA
[2]Astromaterials Research and Exploration Science Division, NASA Johnson Space Center, Houston, TX, USA
[3]Solar System Division, NASA Goddard Space Flight Center, Greenbelt, MD, USA
[4]Department of Geology, Rowan University, Glassboro, NJ, USA
[5]Department of Earth and Planetary Science, American Museum of Natural History, New York, NY, USA
[6]Dust Data Management, Tucson, AZ, USA

Submitted 28 February 2024

Abstract

The Quantitative Reflectance Imaging System (QRIS) is a laboratory-based spectral imaging system constructed to image the sample of asteroid Bennu delivered to Earth by the Origins, Spectral Interpretation, Resource Identification, and Security–Regolith Explorer (OSIRIS–REx) spacecraft. The system was installed in the OSIRIS–REx cleanroom at NASA's Johnson Space Center to collect data during preliminary examination of the Bennu sample. QRIS uses a 12-bit machine vision camera to measure reflectance over wavelength bands spanning the near ultraviolet to the near infrared. Raw data are processed by a calibration pipeline that generates a series of monochromatic, high-dynamic-range reflectance images, as well as band ratio maps, band depth maps, and 3-channel color images. The purpose of these spectral reflectance data is to help characterize lithologies in the sample and compare them to lithologies observed on Bennu by the OSIRIS–REx spacecraft. This initial assessment of lithological diversity was intended to help select the subsamples that will be used to address mission science questions about the early solar system and the origins of life and to provide important context for the selection of representative subsamples for preservation and

Exploring Eco-Friendly Gas Mixtures for Resistive Plate Chambers: A Comprehensive Study on Performance and Aging

The RPC ECOgas@GIF++ Collaboration: L. Quaglia[a], M. Abbrescia[f,c], G. Aielli[u], R. Aly[c,h], M. C. Arena[q], M. Barroso[k], L. Benussi[d], S. Bianco[d], D. Boscherini[g], F. Bordon[p], A. Bruni[g], S. Buontempo[r], M. Busato[p], P. Camarri[u], R. Cardarelli[m], L. Congedo[c], D. De Jesus Damiao[k], M. De Serio[f,c], A. Di Ciaccio[u], L. Di Stante[u], P. Dupieux[n], J. Eysermans[s], A. Ferretti[l,a], G. Galati[f,c], M. Gagliardi[l,a], R. Guida[p], G. Iaselli[b,c], B. Joly[n], S.A. Juks[x], K.S. Lee[w], B. Liberti[m], D. Lucero Ramirez[v], B. Mandelli[p], S.P. Manen[n], L. Massa[g], A. Pastore[c], E. Pastori[m], D. Piccolo[d], L. Pizzimento[m], A. Polini[g], G. Proto[m], G. Pugliese[b,c], D. Ramos[b,c], G. Rigoletti[p], A. Rocchi[m], M. Romano[g], A. Samalan[j], P. Salvini[i], R. Santonico[u], G. Saviano[e], M. Sessa[m], S. Simone[f,c], L. Terlizzi[l,a], M. Tytgat[j,t], E. Vercellin[l,a], M. Verzeroli[o], N. Zaganidis[v]

[a] *INFN Sezione di Torino, Via P. Giuria 1, Torino, 10125, Italy,*
[b] *Politecnico di Bari, Dipartimento Interateneo di Fisica, via Amendola 173, Bari, 70125, Italy,*
[c] *INFN Sezione di Bari, Via E. Orabona 4, Bari, 70125, Italy,*
[d] *INFN - Laboratori Nazionali di Frascati, Via Enrico Fermi 54, Frascati (Roma), 00044, Italy,*
[e] *Sapienza Università di Roma, Dipartimento di Ingegneria Chimica Materiali Ambiente, Piazzale Aldo Moro 5, Roma, 00185, Italy,*
[f] *Università degli studi di Bari, Dipartimento Interateneo di Fisica, Via Amendola 173, Bari, 70125, Italy,*
[g] *INFN Sezione di Bologna, Via C. Berti Pichat 4/2, Bologna, 40127, Italy,*
[h] *Helwan University, , Helwan, Cairo Governorate, 4037120, Egypt,*
[i] *INFN Sezione di Pavia, Via A. Bassi 6, Pavia, 27100, Italy,*
[j] *Ghent University, Dept. of Physics and Astronomy, Proeftuinstraat 86, Ghent, B-9000, Belgium,*
[k] *Universidade do Estado do Rio de Janeiro, R. São Francisco Xavier, 524, Maracanã, Rio de Janeiro - RJ, 20550-013, Brazil,*
[l] *Università degli studi di Torino, Dipartimento di Fisica, Via P. Giuria 1, Torino, 10125, Italy,*
[m] *INFN Sezione di Roma Tor Vergata, Via della Ricerca Scientifica 1, Roma, 00133, Italy,*
[n] *Clermont Université, Université Blaise Pascal, CNRS/IN2P3, Laboratoire de Physique Corpusculaire, BP 10448, Clermont-Ferrand, F-63000, France,*
[o] *Universitè Claude Bernard Lyon I, 43 Bd du 11 Novembre 1918, Villeurbanne, 69100, France,*
[p] *CERN, Espl. des Particules 1, Meyrin, 1211, Switzerland,*
[q] *Università degli studi di Pavia, Corso Strada Nuova 65, Pavia, 27100, Italy,*
[r] *INFN Sezione di Napoli, Complesso universitario di Monte S. Angelo ed. 6 Via Cintia, Napoli, 80126, Italy,*
[s] *Massachusetts Institute of Technology, 77 Massachusetts Ave, Cambridge, MA, 02139, USA,*
[t] *Vrije Universiteit Brussel (VUB-ELEM), Dept. of Physics, Pleinlaan 2, Brussels, 1050, Belgium,*
[u] *Università degli studi di Roma Tor Vergata, Dipartimento di Fisica, Via della Ricerca Scientifica 1, Roma, 00133, Italy,*
[v] *Universidad Iberoamericana, Dept. de Fisica y Matematicas, , Mexico City, 01210, Mexico,*
[w] *Korea University, 145 Anam-ro, Seongbuk-gu, Seoul, , Korea,*
[x] *Université Paris-Saclay, 3 rue Joliot Curie, Bâtiment Breguet, Gif-sur-Yvette, 91190, France,*

Abstract

Resistive Plate Chambers (RPCs) are gaseous detectors widely used in high energy physics experiments, operating with a gas mixture primarily containing Tetrafluoroethane ($C_2H_2F_4$), commonly known as R-134a, which has a global warming potential (GWP) of 1430. To comply with European regulations and explore environmentally friendly alternatives, the RPC EcoGas@GIF++ collaboration, involving ALICE, ATLAS, CMS, LHCb/SHiP, and EP-DT communities, has undertaken intensive R&D efforts to explore new gas mixtures for RPC technology.

A leading alternative under investigation is HFO1234ze, boasting a low GWP of 6 and demonstrating reasonable performance compared to R-134a. Over the past few years, RPC detectors with slightly different characteristics and electronics have been studied using HFO and CO_2-based gas mixtures at the CERN Gamma Irradiation Facility. An aging test campaign was launched in August 2022, and during the latest test beam in July 2023, all detector systems underwent evaluation. This contribution will report the results of the aging studies and the performance evaluations of the detectors with and without irradiation.

Keywords: Resistive Plate Chambers, eco-friendly gas mixtures, aging studies

1. Introduction

Resistive Plate Chambers (RPCs) are gaseous detectors with planar geometry and resistive electrodes (either made out of bakelite or glass). Thanks to their relatively low-cost and ≈ns time resolution they are widely employed in the muon trigger/identification systems of the LHC experiments [1, 2, 3]. These RPCs are operated in avalanche mode, with a gas mixture containing a high fraction (> 90%) of $C_2H_2F_4$ and SF_6 (plus a fraction of i-C_4H_{10} as photon quencher) and, although this mixture satisfies all the performance requirements, it contains a high fraction of $C_2H_2F_4$ and SF_6, which are classified as fluorinated greenhouse gases (F-gases/GHGs).

Starting from 2014, new European Union regulations [4] have imposed a progressive phase-down in the production and usage of these compounds, leading to an increase of cost and reduction in availability. For this reason, CERN has adopted a policy of F-gases reduction and, since RPCs represent a significant fraction of the total GHG-gases emission of the LHC experiments[5], it is of the utmost importance to search for

Radiation Hardness Studies of RPC Based on Diamond-Like Carbon Electrodes for MEG II Experiment

Masato Takahashi[a,*], Sei Ban[b], Weiyuan Li[c], Atsuhiko Ochi[a], Wataru Ootani[b], Atsushi Oya[c], Hiromu Suzuki[a], Kensuke Yamamoto[c]

[a]*Department of Physics, Kobe University, 1-1 Rokkodai-cho, Nada-ku, Kobe, 657-8501, Hyogo, Japan*
[b]*ICEPP, The University of Tokyo, 7-3-1 Hongo, Bunkyo-ku, 113-0033, Tokyo, Japan*
[c]*Department of Physics, The University of Tokyo, 7-3-1 Hongo, Bunkyo-ku, 113-0033, Tokyo, Japan*

Abstract

A novel type of resistive plate chamber, based on diamond-like carbon (DLC) electrodes is under development for background identification in the MEG II experiment. The DLC-RPC is required to have a radiation hardness to mass irradiation since it is planned to be placed in a high-intensity and low-momentum muon beam. In this study, the aging test using a high-intensity X-ray beam was conducted to evaluate the radiation hardness of the DLC-RPC. The accumulated charge due to X-ray irradiation reached about 54 C/cm^2, which is approximately half of the one-year irradiation dose expected in the MEG II experiment. As a result, the degradation of the gas gain was observed due to fluorine deposition and insulators formed on the DLC electrodes. In addition, discharges via spacers were also observed repeatedly and interrupted the DLC-RPC operation.

Keywords: Gaseous detectors, Resistive Plate Chambers, Diamond-Like Carbon, MEG II, Aging studies

1. Introduction

The MEG II experiment [1] searches for $\mu \to e\gamma$ decay, one of the charged lepton flavor violating processes. The dominant background is an accidental coincidence between background γ-rays and background positrons in the MEG II experiment. Identification of the radiative muon decay (RMD; $\mu \to e\nu\bar{\nu}\gamma$), one of the background γ-ray sources, can further suppress background events. A novel type of resistive plate chamber, based on diamond-like carbon (DLC) electrodes is under development and planned to be installed in front of the target for background identification in the MEG II experiment [1]. It detects low-energy positrons of 1 – 5 MeV from the RMD with a high-energy γ-ray of $E_\gamma > 48$ MeV. The detector should have an ultra-low mass (0.1 % X_0), high-rate capability (up to 3 MHz/cm^2), and radiation hardness (irradiation dose of ~ 100 C/cm^2) since the high-intensity (7×10^7 μ/s) and low-momentum (28 MeV/c) muon beam pass through there. Furthermore, the detection efficiency of 90 % for minimum ionizing particles, the timing resolution of 1 ns, and the 20 cm diameter detector size are also required to identify the RMD efficiently.

The DLC-RPC consists of thin-film materials as shown in Fig. 1. The overall material budget can be suppressed to 0.095 % X_0 with a four-layer configuration. A single-layer detection efficiency is required to be above 44 % to achieve the 90 % detection efficiency with a four-layer configuration. Some requirements for the DLC-RPC, which rate capability, detection efficiency, and timing resolution in a high-intensity and low-momentum

*Corresponding author
Email address: m.takahashi@stu.kobe-u.ac.jp (Masato Takahashi)

Search for Axion dark matter with the QUAX–LNF tunable haloscope

A. Rettaroli,[1,*] D. Alesini,[1] D. Babusci,[1] C. Braggio,[2,3] G. Carugno,[2] D. D'Agostino,[4,5] A. D'Elia,[1] D. Di Gioacchino,[1] R. Di Vora,[6] P. Falferi,[7,8] U. Gambardella,[4,5] C. Gatti,[1] G. Iannone,[4,5] C. Ligi,[1] A. Lombardi,[6] G. Maccarrone,[1] A. Ortolan,[6] G. Ruoso,[6] S. Tocci,[1,†] and G. Vidali[9,1]

[1] *INFN, Laboratori Nazionali di Frascati, Frascati, Roma, Italy*
[2] *INFN, Sezione di Padova, Padova, Italy*
[3] *Dipartimento di Fisica e Astronomia, Padova, Italy*
[4] *Dipartimento di Fisica E.R. Caianiello, Fisciano, Salerno, Italy*
[5] *INFN, Sezione di Napoli, Napoli, Italy*
[6] *INFN, Laboratori Nazionali di Legnaro, Legnaro, Padova, Italy*
[7] *Istituto di Fotonica e Nanotecnologie, CNR Fondazione Bruno Kessler, I-38123 Povo, Trento, Italy*
[8] *INFN, TIFPA, Povo, Trento, Italy*
[9] *Dipartimento di Fisica, Università La Sapienza, Rome, Italy*

(Dated: March 1, 2024)

We report the first experimental results obtained with the new haloscope of the QUAX experiment located at Laboratori Nazionali di Frascati of INFN (LNF). The haloscope is composed of a OFHC Cu resonant cavity cooled down to about 30 mK and immersed in a magnetic field of 8 T. The cavity frequency was varied in a 6 MHz range between 8.831496 and 8.83803 GHz. This corresponds to a previously unprobed mass range between 36.52413 and 36.5511 μeV. We don't observe any excess in the power spectrum and set limits on the axion-photon coupling in this mass range down to $g_{a\gamma\gamma} < 0.861 \times 10^{-13}$ GeV^{-1} with the confidence level set at 90%.

I. INTRODUCTION

In recent years, we witnessed an increasing growth in the research of light Dark Matter (DM) candidates, addressing in particular axions and axion-like particles (ALPs). If axions are found to exist, they would untie the long-standing DM problem [1, 2], after being originally postulated as a solution to the strong CP problem [3, 4]. The nature of a pseudoscalar, electrically neutral and feebly interacting particle make the axion a strong DM candidate [5], and its cosmological evolution and astrophysical constraints indicate a favorable mass range between 1 μeV $< m_a <$ 10 meV [6].

The research efforts are now spread over many different detection approaches, but the paradigm has become the haloscope design proposed by Sikivie [7, 8], which probes axions from the DM halo of the Galaxy. Currently operating haloscopes are ADMX [9–12], HAYSTAC [13, 14], ORGAN [15], CAPP-8T [16, 17], CAPP-9T [18], CAPP-PACE [19], CAPP-18T [20], CAST-CAPP [21], GrAHal [22], RADES [23–25], TASEH [26] and QUAX [27–32], whereas among the proposed experiments are FLASH [33], ABRACADABRA [34], DM-Radio [35, 36], CADEx [37], MADMAX [38] and ALPHA [39].

The axion observation technique is based upon its inverse Primakoff conversion into one photon, stimulated by a static magnetic field. The essential elements required to run a haloscope are a superconducting magnet to generate a strong magnetic field, a microwave resonant cavity where the electromagnetic field excitation builds up, an ultra-low noise receiver, a tuning mechanism to scan over the axion mass range and a cryogenic system to grant operation at low temperature. The two figures of merit in the axion search are the power of the produced photon [40]

$$P_{a\gamma} = \left(\frac{g_{a\gamma\gamma}^2}{m_a^2}\hbar^3 c^3 \rho_a\right)\left(\frac{\beta}{1+\beta}\omega_c \frac{1}{\mu_0} B_0^2 V C_{010} Q_L\right) \times \left(\frac{1}{1+(2Q_L\,\Delta_\omega/\omega_c)^2}\right), \tag{1}$$

and the scan rate [41]

$$\frac{\mathrm{d}f}{\mathrm{d}t} = g_{a\gamma\gamma}^4 \frac{\rho_a^2}{m_a^2}\frac{1}{\mathrm{SNR}^2}\left(\frac{B_0^2 V C_{010}}{k_B T_{\mathrm{sys}}}\right)^2 \times \frac{\beta^2}{(1+\beta)^2} Q_a \min\left(Q_L, Q_a\right). \tag{2}$$

We assume a local DM density $\rho_a = 0.45$ GeV/cm^3 [42], m_a is the axion mass and $g_{a\gamma\gamma}$ is its coupling constant to photons. B_0 is the applied magnetic field; $\omega_c = 2\pi\nu_c$, V, Q_L, β are respectively the resonance angular frequency of the cavity, the volume, the loaded quality factor and the antenna coupling to the cavity. The relation $Q_L = Q_0/(1+\beta)$ holds, with Q_0 the intrinsic quality factor. C_{010} is a mode dependent geometrical factor, about 0.6 for the TM010 resonant mode of a cylindrical cavity, and $\Delta\omega_c = \omega_c - \omega_a$ is the detuning between the cavity and the axion angular frequency defined as $\omega_a = m_a c^2/\hbar$. The quality factor $Q_a \approx 10^6$ [43] is related to the energy spread in the cold dark matter halo. In Eq. 2, the signal-to-noise ratio, SNR, is defined as the ratio between the signal power and the uncertainty of

* alessio.rettaroli@lnf.infn.it
† simone.tocci@lnf.infn.it

Aging effects in the COMPASS hybrid GEM-Micromegas pixelized detectors

Damien Neyret[1,*], Philippe Abbon[1], Marc Anfreville[1,†], Vincent Andrieux[2], Yann Bedfer[1], Dominique Durand[1], Sébastien Herlant[1], Nicole d'Hose[1], Fabienne Kunne[1], Stephane Platchkov[1], Florian Thibaud[1], Michel Usseglio[1], Maxence Vandenbroucke[1]

[1] *CEA IRFU, Université Paris-Saclay, 91191 Gif sur Yvette Cedex, France*

[2] *University of Illinois at Urbana-Champaign, Dept. of Physics, Urbana, IL 61801-3080, USA*

Proceedings to the 3rd International Conference on Detector Stability and Aging Phenomena in Gaseous Detectors, CERN, November 6-10 2023

Abstract

Large-size hybrid and pixelized GEM-Micromegas gaseous detectors (40x40 cm² active area) were developed and installed in 2014 and 2015 for the COMPASS2 physics program which started at the same time. That program involved in particular two full years of Drell-Yan studies using a high-intensity pion beam on a thick polarized target. Although the detectors were placed behind a thick absorber, they were exposed to an important flux of low energy neutrons and photons. The detectors were designed to drastically reduce the discharge rate, a major issue for non-resistive Micromegas in high hadron flux, by a factor of more than 100 compared to the former ones. A hybrid solution was chosen where a pre-amplifying GEM foil is placed 2 mm above the micromesh electrode. A pixelized readout was also added in the center of the detector, where the beam is going through, in order to track particles scattered at very low angles. The combination of the hybrid structure and the pixelized central readout allowed the detector to be operated in an environment with particle flux above 10 MHz/cm² with very good detection efficiencies and spatial resolution. The performance has remained stable since 2015 in terms of gain and resolution, showing the interest of hybrid structures associating a GEM foil to a Micromegas board to protect gaseous detectors against discharges and aging effects

Keywords: Micromegas hybrid detectors, Micro-patterned Gaseous Detectors (MPGD), Detector efficiency, Spatial resolution, Detector aging study, COMPASS experiment

1. Introduction

The first detectors based on the Micromegas technology [1] were developed and optimized in the late 90's. They were used in the COMPASS experiment at CERN as trackers for particles scattered at small angle [2]. They were placed right after the target, where the particle flux is the largest, and designed to track charged particles at a radial distance from the beam from 2.5 up to 20 cm, on a surface of 40x40 cm². Twelve planes were installed on 3 stations, consisting of 4 detectors in 4 different orientations X, Y, U and V (respectively 0°, 90° and ±45°). They were using a gas mixture of Neon with 10% ethane and 10% of CF_4. These detectors were installed in 2001-2002 at the very beginning of the experiment, and showed excellent performance with muon beams in terms of efficiency and spatial and time resolutions. When used with hadron beams the relatively high sparking rate of the Micromegas detectors required to reduce the gain and to remove the CF_4 component from the gas mixture, leading to a slight decrease of the detector performance.

In anticipation for the second phase of the COMPASS experiment [3] [4], an upgrade of the Micromegas detectors was necessary with two main objectives: to increase the ability to operate in high hadron flux, and to make the new detectors active in their center, unlike in the first generation. An R&D was pursued in 2008-2013 in order to reach these objectives. New pixelized hybrid Micromegas detectors [5] were developed, built and installed in the COMPASS spectrometer in 2014-2015, with excellent performance. These detectors have been used on the COMPASS experiment until its termination at end of 2022. They were used since 2023 on the AMBER experiment [6].

* Corresponding author, email: damien.neyret@cea.fr

† Deceased

Stability studies of sealed Resistive Plate Chambers

A. Blanco[a], P. Fonte[a,b], L. Lopes[a,*], M. Pimenta[a,c]

[a]*Laboratório de Instrumentação e Física Experimental de Partículas (LIP), Departamento de Física da Universidade de Coimbra, 3004-516 Coimbra, Portugal*
[b]*Instituto Politécnico de Coimbra, Instituto Superior de Engenharia de Coimbra, Rua Pedro Nunes, 3030-199 Coimbra, Portugal*
[c]*Departamento de Física, Instituto Superior Técnico, Universidade de Lisboa Avenida Rovisco Pais, n. 1, 1049-001 Lisboa, Portugal*

Abstract

The phase-out of hydro-fluorocarbons, owing to their high Global Warming Power, affecting the main gas used in Resistive Plate Chambers (RPCs), tetrafluoroethane $C_2H_2F_4$, has increased operational difficulties on existing systems and imposes strong restrictions on its use in new systems.

This has motivated a new line of R&D on sealed RPCs: RPCs that do not require a continuous gas flow for their operation and dispense the use of very complex and expensive re-circulation and/or recycling gas systems. At the moment it is not clear whether this solution can cover all fields of application normally allocated to RPCs, but it seems that it could be considered as a valid option for low particle flux triggering/tracking of particles, e.g. in cosmic ray or rare event experiments.

In this work, we demonstrate the feasibility of a small telescope for atmospheric muon tracking consisting of four 300 x 300 mm^2 sealed RPCs with gas gap widths of 1 mm, 1.5 mm and 2 mm. The results suggest that it is possible to operate this type of detectors for extended periods of time (more than five months) with its main characteristics, efficiency, average charge and streamer probability, without apparent degradation and similar to a RPC operated in continuous gas flow.

Keywords: Gaseous detectors; Sealed RPC; HFCs phase-out;

1. Introduction

Resistive Plate Chambers (RPC), like most gaseous detectors, rely on the purity of the gas to keep their performance stable. For this reason, they operate with re-circulation, purification and cleaning systems that attempt to keep the gas purity unchanged. Gas purity degradation is, in the first instance, primarily due to leaks/permeability in the system that allow atmospheric gases and/or humidity to enter, as well as the release of hydrofluorocarbons (HFCs), with $C_2H_2F_4$ as main constituent. This results in the need to inject substantial amounts of fresh gas. The use of HFCs, and in particular their release into the environment, is a serious problem today. This is due to the high global warming potential (GWP) of HFCs, which contributes significantly to global warming. In fact, the European Union (EU) decreed, already in 2015, the phase-out of HFCs. This poses serious problems for existing RPC systems, but especially for new systems, which will certainly not be able to be planned in the same way. In addition, the gas system associated with these detectors introduces considerable complexity and cost.

A possible solution to the problem, from an environmental point of view (the problem of the complexity of the gas system would remain), is the replacement of these gases by others with a much lower GWP, the so-called green gases [1], with HFO-1234ze ($C_3H_2F_4$) as the most promising solution [2].

Another possible solution would be to construct and operate RPCs without any gas supply, i.e. RPCs that contain gas but are hermetically sealed after construction, similar to the popular Geiger-Mueller tube. This concept has been baptized as sealed RPCs (sRPC) [3, 4]. It would mitigate the problem of HFCs phasing out by drastically minimizing (by orders of magnitude) the amount of gas used today, reducing its environmental impact to negligible levels. It would also eliminate any dependence on complex gas systems, allowing the expansion of this type of technology towards Cosmic Ray (CR) experiments through the construction of large, high-performance arrays at low cost, which would replace the simple Cerenkov water tanks in remote and difficult-to-access locations typical of CR experiments [5].

In this work, we present the characterization and stability studies of four 300 x 300 mm^2 sRPCs with gas gap widths of 1 mm, 1.5 mm and 2 mm, by exposing them to the natural flux of cosmic rays.

2. Experimental setup

2.1. Sealed RPC modules

The sRPC modules are multi-gap structures [6] equipped with two gas gaps defined by three 2 mm thick soda lime glass electrodes [1] of about 350 x 350 mm^2 separated by spacers. Each gap includes a circular spacer made of a soda lime glass

*Corresponding authors
Email addresses: alberto@coimbra.lip.pt (A. Blanco), luisalberto@coimbra.lip.pt (L. Lopes)

[1] with bulk resistivity of $\approx 5x10^{12}$ Ωcm at 25 °C

Investigation of full-charm and full-bottom pentaquark states

K. Azizi*
Department of Physics, University of Tehran, North Karegar Avenue, Tehran 14395-547, Iran
Department of Physics, Doğuş University, Dudullu-Ümraniye, 34775 Istanbul, Turkey and
School of Particles and Accelerators, Institute for Research in Fundamental Sciences (IPM) P.O. Box 19395-5531, Tehran, Iran

Y. Sarac†
Electrical and Electronics Engineering Department, Atilim University, 06836 Ankara, Turkey

H. Sundu‡
Department of Physics Engineering, Istanbul Medeniyet University, 34700 Istanbul, Turkey
(Dated: March 1, 2024)

The continuous advancement of experimental techniques and investigations has led to observations of various exotic states in particle physics. Each addition to this family of states not only raises expectations for future discoveries but also focuses attention on such potential new states. Building upon this motivation and inspired by recent observations of various traditional and exotic particles containing an increased number of heavy quarks, our study provides a spectroscopic search for potential pentaquark states with spin-parity $\frac{3}{2}^-$ and composed entirely of charm or bottom quarks. We predict the masses for full-charm and full-bottom pentaquark states as $m = 7628 \pm 112$ MeV and $m = 21982 \pm 144$ MeV, respectively. We also compute the current couplings of these states to vacuum, which are main inputs in investigations of their various possible decays.

I. INTRODUCTION

Since the proposal of the quark model, hadrons with non-conventional structures, which do not fit the conventional baryons composed of three quarks (antiquarks) and mesons composed of a quark and an antiquark, have been subjects of interests. The theory of strong interaction does not rule out the existence of such states, and this has attracted interest in these states. They were investigated extensively in both theory and experiments. Finally, the first evidence came out with the observation of $X(3872)$ state in 2003 [1]. And following this observation, many other such exotic state candidates were observed [2–10] and listed in Particle Data Group (PDG) [11]. These observations were also followed by many theoretical investigations trying to explain their internal structures, which still have ambiguity and need to be clearly identified with more scrutiny. It is evident that we will come across with other such possible exotic states in the future. This expectation necessitates their examinations in detail via different approaches to provide an understanding of their substructure and properties and provide feedback for future investigations. Besides, these states help to deepen our understanding of the dynamics of the strong interaction.

The pentaquark states are among these non-conventional states with their first observation reported in 2015 by the LHCb collaboration [3]. The investigation of the $\Lambda_b^0 \to J/\psi p K^-$ process resulted in two pentaquark states in the $J/\psi p$ invariant mass spectrum with the following resonance parameters [3]: $m_{P_c(4380)^+} = 4380 \pm 8 \pm 29$ MeV, $\Gamma_{P_c(4380)^+} = 205 \pm 18 \pm 86$ MeV and $m_{P_c(4450)^+} = 4449.8 \pm 1.7 \pm 2.5$ MeV, $\Gamma_{P_c(4450)^+} = 39 \pm 5 \pm 19$ MeV. This observation was supported by a full amplitude analysis for $\Lambda_b^0 \to J/\psi p \pi^-$ decays [4] in 2016. In 2019, using updated data, a new pentaquark state, $P_c(4312)^+$, was reported with $m_{P_c(4312)^+} = 4311.9 \pm 0.7^{+6.8}_{-0.6}$ MeV and $\Gamma_{P_c(4312)^+} = 9.8 \pm 2.7^{+3.7}_{-4.5}$ MeV by the LHCb collaboration and analyses revealed two narrow overlapping peaks for the previously observed peak of the $P_c(4450)^-$ state with masses and widths: $m_{P_c(4440)^+} = 4440.3 \pm 1.3^{+4.1}_{-4.7}$ MeV, $\Gamma_{P_c(4440)^+} = 20.6 \pm 4.9^{+8.7}_{-10.1}$ MeV and $m_{P_c(4457)^+} = 4457.3 \pm 0.6^{+4.1}_{-1.7}$ MeV, $\Gamma_{P_c(4457)^+} = 6.4 \pm 2.0^{+5.7}_{-1.9}$ MeV [5]. In the recent investigations, new states with the strange quark were also added to this family. The LHCb collaboration reported the $P_{cs}(4459)^0$ state through the investigation of $J\psi\Lambda$ invariant mass distribution in $\Xi_b^- \to J/\psi K^- \Lambda$ decays [9]. The mass and width for the $P_{cs}(4459)^0$ were given as $m = 4458.8 \pm 2.9^{+4.7}_{-1.1}$ MeV, and $\Gamma = 17.3 \pm 6.5^{+8.0}_{-5.7}$ MeV [9]. $P_{cs}(4338)$ state was reported with the mass $4338.2 \pm 0.7 \pm 0.4$ MeV and the width $7.0 \pm 1.2 \pm 1.3$ MeV from the amplitude analyses of $B^- \to J/\psi \Lambda \bar{p}$ [10].

Following the observations of the above pentaquark states, theoretical researches chasing the purpose of identifying their various properties have focused on these states. The sub-structures and quantum numbers of these observed

* kazem.azizi@ut.ac.ir; Corresponding author
† yasemin.sarac@atilim.edu.tr
‡ hayriyesundu.pamuk@medeniyet.edu.tr

New Physics with PeV Astrophysical Neutrino Beams

By

Ibrahim Safa

A dissertation submitted in partial fulfillment of

the requirements for the degree of

Doctor of Philosophy

(Physics)

at the

University of Wisconsin – Madison

2022

Date of final oral examination: August 17, 2022

The dissertation is approved by the following members of the Final Oral Committee:

Francis Halzen, Professor, Physics

Carlos Argüelles, Assistant Professor, Physics

Ke Fang, Assistant Professor, Physics

Amy Barger, Professor, Astronomy

Benjamin Jones, Professor, Physics

Abstract

Astrophysical neutrinos allow us to access energies and baselines that cannot be reached by human-made accelerators, offering unique probes of new physics phenomena. This thesis aims to address the challenges currently facing searches for Beyond Standard Model (BSM) physics in the high-energy universe using astrophysical neutrinos, particularly in the contexts of flavor measurements and connections with dark matter.

The search for new physics with astrophysical neutrinos requires as a prerequisite understanding standard neutrino sources, which remain ambiguous. We begin by performing a multi-wavelength search for astrophysical neutrino sources using nine years of IceCube data. We find hints of neutrino emission from radio-bright Active Galactic Nuclei (AGN), further supporting recent claims that neutrino emission occurs near the core of AGNs.

Next we turn our attention to BSM searches. Accurate flavor measurements of the astrophysical flux provide a smoking gun signature to BSM physics. This requires a precise measurement of the tau neutrino fraction. However, tau identification proved a major hurdle in the current generation of observatories. We confront the problem of astrophysical neutrino flavor measurements by first introducing `TauRunner`, a simulation tool that accurately models the propagation of tau neutrinos including previously neglected effects such as tau lepton energy losses and depolarization in matter. We show that better modeling of tau neutrino propagation improves IceCube transient point-source sensitivities by more than an order of magnitude at EeV energies, and diffuse flux sensitivities by a factor of two. Second, we use this software to model IceCube counterparts to anomalous events reported by the ANITA experiment. After performing an analysis using IceCube data, we show that all Standard Model explanations are ruled out. Looking ahead to the future of flavor measurements, we also present a study that predicts the production of tau neutrinos via the propagation of electron and muon neutrinos in Earth, finding an irreducible but quantifiable background to next-generation tau neutrino observatories.

Finally, we attempt to address the field's shared ignorance of the origin of neutrino and dark matter masses by exploring potential connections between the two. Specifically, we present an analysis of dark matter annihilation and decay to neutrinos. We obtain limits from MeV to ZeV masses using more than a dozen neutrino experiments. Notably, using recent data from the SuperKamiokande experiment, we place the first-ever limit on dark matter annihilation that reaches

Deciphering the Belle II data on $B \to K\nu\bar{\nu}$ decay in the (dark) SMEFT with minimal flavour violation

Biao-Feng Hou,[a] **Xin-Qiang Li,**[a,b] **Meng Shen,**[a] **Ya-Dong Yang**[a,c] **and Xing-Bo Yuan**[a]

[a] *Institute of Particle Physics and Key Laboratory of Quark and Lepton Physics (MOE), Central China Normal University, Wuhan, Hubei 430079, China*

[b] *Center for High Energy Physics, Peking University, Beijing 100871, China*

[c] *Institute of Particle and Nuclear Physics, Henan Normal University, Xinxiang 453007, China*

E-mail: resonhou@zknu.edu.cn, xqli@ccnu.edu.cn, shenmeng@mails.ccnu.edu.cn, yangyd@ccnu.edu.cn, y@ccnu.edu.cn

Abstract: Recently, the Belle II collaboration announced the first measurement of the branching ratio $\mathcal{B}(B^+ \to K^+\nu\bar{\nu})$, which is found to be about 2.7σ higher than the Standard Model (SM) prediction. We decipher the data with two new physics scenarios: the underlying quark-level $b \to s\nu\bar{\nu}$ transition is, besides the SM contribution, further affected by heavy new mediators that are much heavier than the electroweak scale, or amended by an additional decay channel with undetected light final states like dark matter or axion-like particles. These two scenarios can be most conveniently analyzed in the SM effective field theory (SMEFT) and the dark SMEFT (DSMEFT) framework, respectively. We consider the flavour structures of the resulting effective operators to be either generic or satisfy the minimal flavour violation (MFV) hypothesis, both for the quark and lepton sectors. In the first scenario, once the MFV assumption is made, only one SM-like low-energy effective operator induced by the SMEFT dimension-six operators can account for the Belle II excess, the parameter space of which is, however, excluded by the Belle upper bound of the branching ratio $\mathcal{B}(B^0 \to K^{*0}\nu\bar{\nu})$. In the second scenario, it is found that the Belle II excess can be accommodated by 22 of the DSMEFT operators involving one or two scalar, fermionic, or vector dark matters as well as axion-like particles. These operators also receive dominant constraints from the $B^0 \to K^{*0} + \text{inv}$ and $B_s \to \text{inv}$ decays. Once the MFV hypothesis is assumed, the number of viable operators is reduced to 14, and the $B^+ \to \pi^+ + \text{inv}$ and $K^+ \to \pi^+ + \text{inv}$ decays start to put further constraints on them. Within the parameter space allowed by all the current experimental data, the q^2 distributions of the $B \to K^{(*)} + \text{inv}$ decays are then studied for each viable operator. We find that the resulting prediction of the operator $\mathcal{Q}_{q\chi} = \left(\bar{q}_p\gamma_\mu q_r\right)\left(\bar{\chi}\gamma^\mu\chi\right)$ with a fermionic dark matter mass $m_\chi \approx 700\,\text{MeV}$ can closely match the Belle II event distribution in the bins $2 \le q^2 \le 7\,\text{GeV}^2$. In addition, the future prospects at Belle II, CEPC and FCC-ee are also discussed for some of these FCNC processes.

Slicing Pomerons in ultraperipheral collisions using forward neutrons from nuclear breakup

M. Alvioli,[1,2] V. Guzey,[3] and M. Strikman[4]

[1] *Consiglio Nazionale delle Ricerche, Istituto di Ricerca per la Protezione Idrogeologica, via Madonna Alta 126, I-06128, Perugia, Italy*
[2] *Istituto Nazionale di Fisica Nucleare, Sezione di Perugia, via Pascoli 23c, I-06123, Perugia, Italy*
[3] *University of Jyvaskyla, Department of Physics, P.O. Box 35, FI-40014 University of Jyvaskyla, Finland and Helsinki Institute of Physics, P.O. Box 64, FI-00014 University of Helsinki, Finland*
[4] *Pennsylvania State University, University Park, PA, 16802, USA*

(Dated: March 1, 2024)

We argue that measurements of forward neutrons from nuclear breakup in inclusive high energy photon-nucleus (γA) scattering provide a novel complementary way to study small-x dynamics of QCD in heavy-ion ultraperipheral collisions (UPCs). Using the leading twist approximation to nuclear shadowing, we calculate the distribution over the number of evaporation neutrons produced in γPb collisions at the LHC. We demonstrate that it allows one to determine the distribution over the number of wounded nucleons (inelastic collisions), which constrains the mechanism of nuclear shadowing of nuclear parton distributions.

PACS numbers:
Keywords: Heavy-ion scattering, ultraperipheral collisions, nuclear shadowing

I. INTRODUCTION AND MOTIVATION

Understanding of the QCD dynamics of hard high energy interactions and the structure of nuclei and nucleons is one of the main directions of theoretical and experimental studies at the Large Hadron Collider (LHC) and the Relativistic Heavy Ion Collider (RHIC). Of particular interest is the limit of very small momentum fractions x, when the linear Dokshitzer-Gribov-Lipatov-Altarelli-Parisi (DGLAP) approximation is expected to break down [1, 2] and a regime close to the black disk limit (BDL) [3] may set in. Its observation is one of the prime objectives of the planned Electron-Ion Collider (EIC) at Brookhaven National Laboratory [4, 5], which will ultimately reach $x \sim 10^{-3}$ for momentum transfers of a few GeV. At the same time, it was pointed out some time ago that ultraperipheral collisions (UPCs) of two ions at the LHC, where a photon emitted by one of the nuclei interacts with the other nucleus, allow one to probe down to $x \sim 10^{-5} - 10^{-4}$, depending on a particular reaction channel and the detector geometry [6, 7].

Electron-nucleus collisions at the EIC and UPCs of heavy ions at the LHC present two options for studying small-x dynamics, which are largely complementary. At the LHC practically all data are collected for one heavy nucleus and one cannot directly access the dependence of cross sections on the virtuality of the probe. At the same time, one can reach very small x, which is provided by a wide rapidity coverage of the LHC detectors and the large invariant photon-nucleus collision energies exceeding by a factor of 100 the design energies at the EIC.

Over the last decade the data taken in the LHC and RHIC kinematics discovered a significant nuclear suppression of coherent J/ψ photoproduction in Pb-Pb and Au-Au UPCs compared to the impulse approximation prediction [8–17]. When interpreted in the leading twist approximation (LTA) [18], it amounts to strong gluon nuclear shadowing [19, 20]:

$$R_A^g(x,Q^2) = \frac{g_A(x,Q^2)}{A g_N(x,Q^2)} < 1\,, \tag{1}$$

where $g_A(x,Q^2)$ and $g_N(x,Q^2)$ are the nucleus and nucleon gluon densities, respectively. Typical numbers reported by the LHC experiments [8–16] correspond to

$$\begin{aligned} R_{\rm Pb}^g(x=10^{-3}, Q^2_{\rm eff}=3\,{\rm GeV}^2) &\approx 0.6\,,\\ R_{\rm Pb}^g(x=10^{-4}, Q^2_{\rm eff}=3\,{\rm GeV}^2) &\approx 0.5\,, \end{aligned} \tag{2}$$

with a similar suppression extending down to $x \sim 10^{-5}$. Here $Q_{\rm eff}$ is the effective resolution scale determined by the charm quark mass. These values of $R_{\rm Pb}^g$ agree very well with the LTA predictions for nuclear shadowing made more than 10 years ago [18]. Note that this interpretation of the J/ψ UPC data is complicated at the next-to-leading order (NLO) of the perturbative expansion in powers of $\log Q^2$ (perturbative QCD) due to large cancellations between the leading-order (LO) and NLO gluon terms, which leaves a numerically important quark contribution [21, 22]. A way to

Light quarkonium hybrid mesons

B. Barsbay,[1] K. Azizi,[2,3,4,*] and H. Sundu[5]

[1]*Division of Optometry, School of Medical Services and Techniques, Doğuş University, 34775 Istanbul, Türkiye*
[2]*Department of Physics, University of Tehran, North Karegar Ave. Tehran 14395-547, Iran*
[3]*Department of Physics, Doğuş University, Dudullu-Ümraniye, 34775 Istanbul, Türkiye*
[4]*School of Particles and Accelerators, Institute for Research in Fundamental Sciences (IPM) P.O. Box 19395-5531, Tehran, Iran*
[5]*Department of Physics Engineering, Istanbul Medeniyet University, 34700 Istanbul, Türkiye*

(Dated: March 1, 2024)

We investigate the light quarkonium hybrid mesons of various spin-parities in QCD. Considering different interpolating currents made of the valence light quarks and single gluon, we calculate the mass and current coupling of the strange and nonstrange members of light hybrid mesons by including into computations the nonperturbative quark and gluon condensates up to ten dimensions in order to increase the accuracy of the results. The obtained results may be useful for future experimental searches of these hypothetical states. They can also be used in the calculations of different parameters related to the decays/interactions of light hybrid mesons to/with other states.

I. INTRODUCTION

As successful theory of strong interaction, the quantum chromodynamics (QCD) together with the powerful quark model have predicted the existence of exotic hadrons beyond the standard mesons and baryons. The most known categories for exotic hadrons are tetraquarks, pentaquarks, hexaquarks, quark-gluon hybrids and glueballs. Starting from 2003, many tetraquark and pentaquark states have been discovered in the experiment. Concerning the hexaquarks, WASA-at-COSY collaboration has reported observation of a six-quark candidate $d^*(2380)$ with $J^P = 3^+$ [1], starting a wide research on the properties of hexaquarks and dibaryons as interesting objects: a hypothetical SU(3) flavor-singlet, highly symmetric, deeply bound neutral particle termed the scalar hexaquark $S = uuddss$ has been introduced as a potential candidate for dark matter [2]. Although some resonances have been introduced as the potential condidates for the hybrids and glueballs, there is no discovered particles with high confidence level in these categories yet. It is time to investigate the hybrid states and glueballs with a fresh breath, though they are searched for a long time. Hybrid states was predicted in 1976 [3]. There are some states with quantum numbers $J^{PC} = 0^{--}$, 0^{+-}, 1^{-+}, 2^{-+}, which cannot be explained by $q\bar{q}$ picture and are considered as potential hybrid meson candidates [4]. Among them are $\pi_1(1400)$ [5], $\pi_1(1600)$ [6], $\pi_1(2015)$ [7], and $\eta_1(1855)$ [8] with exotic quantum numbers $J^{PC} = 1^{-+}$ evidenced by some experiments. They are possible single-gluon hybrid candidates of a quark-antiquark pair together with a valence gluon. Designed to search for the hybrid mesons as its primary goal, the GlueX experiment at Jefferson Lab is expected to give crucial insights into the existence and structure of the exotic hybrid mesons.

Investigation of the light and heavy hybrid mesons is of great importance not only for determination of their nature and quark-gluon organization but for gaining useful information about the nonperturbative nature of QCD. Light hybrid states, which are subjects of the present study, have been intensively investigated in the framework of different theoretical methods such as lattice QCD [9, 10], the Schwinger-Dyson formalism [11–13],the flux tube model [14, 15], the MIT bag model [16, 17] and QCD Laplace sum-rules(LSRs) [18–34]. In particular, Ref. [21] contains a comprehensive LSRs analysis of the light hybrids for $J = 0$ and 1 with all the possible combinations for the parity and charge quantum numbers. Analyses show that the 0^{++}, 0^{--}, 1^{++}, and 1^{--} states are mainly stable, while 0^{+-}, 0^{-+}, 1^{+-}, and 1^{-+} quantum numbers lead to unstable and controversial results. Expected to be the lightest hybrid mesons, the ones with 1^{-+} have been the subject of much additional studies. In the QCD sum rules, predictions on the 1^{-+} light hybrid mesons are inconsistent among different works. For instance, I. I. Balitsky *et al*'s prediction of mass for 1^{-+} state is in the range, 1.0–1.3 GeV [18, 22], J . I. Latorre *et al* predicted the related mass to be around 2.1 GeV [24] and the obtained mass for 1^{-+} state is around 2.5 GeV in Refs. [19, 35, 36]. The mass of 1^{-+} was re-analyzed by including the quark-gluon condensates up to 8 dimensions [34] and it was found that the mass value increases to be in the range 1.72–2.60 GeV. The obtained mass range did not favor the $\pi_1(1400)$ and the $\pi_1(1600)$ to be pure hybrid states and suggests the $\pi_1(2015)$, observed by E852, to have much of a hybrid constituent. The masses of the light hybrid mesons with $J^{PC} = 1^{-+}$ quantum numbers have also been calculated using different theoretical methods other than QCD sum rules [37–40].

Concerning other quantum numbers, the masses of the 0^{++} and 0^{-+} light hybrid mesons were calculated using the QCD sum rule method by considering two kinds of the interpolated currents with the same quantum numbers. While the approximately equal mass was predicted for the 0^{-+} hybrid states from the two different currents, different masses were obtained for the 0^{++} hybrid

*Corresponding Author

Revealing the nature of Ω_c-like states from pentaquark perspective

Ulaş Özdem[1, *]

[1] *Health Services Vocational School of Higher Education, Istanbul Aydin University, Sefakoy-Kucukcekmece, 34295 Istanbul, Türkiye*

(Dated: March 1, 2024)

We systematically study the electromagnetic properties of controversial states whose internal structure is not elucidated and we try to offer a different point of view to unravel the internal structure of these states. Inspired by the Ω_c states observed by the LHCb Collaboration, we study the electromagnetic properties of the Ω_c-like states as the compact diquark-diquark-antiquark pentaquarks with both $J^P = \frac{1}{2}^-$ and $J^P = \frac{3}{2}^-$ in the context of the QCD light-cone sum rule model. From the obtained numerical results, we conclude that the magnetic dipole moments of the Ω_c-like states can reflect their inner structures, which can be used to distinguish their spin-parity quantum numbers. Measuring the magnetic moment of the Ω_c-like states in future experimental facilities can be very helpful for understanding the internal organization and identifying the quantum numbers of these states.

Keywords: Electromagnetic form factors, diquark-diquark-antiquark picture, QCD light-cone sum rules, magnetic dipole moments

I. MOTIVATION

Many heavy baryon states have been discovered in recent years by experimental collaborations. One of the main challenges in non-perturbative QCD is to understand and shed light on the precise nature of these states. Through further theoretical explorations involving the study of hadrons comprising a single heavy quark, it offers an exquisite basis to probe the dynamics of a light diquark in a heavy quark background, to enhance the understanding of the non-perturbative nature of QCD, and to test the predictions of different phenomenological models. In recent decades, there have been significant experimental advancements in the field of singly-charm/bottom baryons, resulting in a dramatic increase in the number of particles [1–30]. As the data for the presence of some of these states is scarce and their internal structure, as well as quantum numbers, are not well defined, additional experimental exploration is therefore required. Therefore, researchers in hadron physics continue to study these topics through theoretical and experimental research, as they have not yet been fully understood.

In 2017, the LHCb collaboration studied the $\Xi_c^+ K^-$ mass spectrum and observed five new narrow excited Ω_c states, $\Omega_c(3000)$, $\Omega_c(3050)$, $\Omega_c(3066)$, $\Omega_c(3090)$, $\Omega_c(3119)$ [22]. The parameters that have been measured are as follows

$$\begin{aligned}
M_{\Omega_c(3000)} &= 3000.4 \pm 0.2 \pm 0.1 \text{ MeV}, \quad \Gamma_{\Omega_c(3000)} = 4.5 \pm 0.6 \pm 0.3 \text{ MeV}, \\
M_{\Omega_c(3050)} &= 3050.2 \pm 0.1 \pm 0.1 \text{ MeV}, \quad \Gamma_{\Omega_c(3050)} = 0.8 \pm 0.2 \pm 0.1 \text{ MeV}, \\
M_{\Omega_c(3066)} &= 3065.6 \pm 0.1 \pm 0.3 \text{ MeV}, \quad \Gamma_{\Omega_c(3066)} = 3.5 \pm 0.4 \pm 0.2 \text{ MeV}, \\
M_{\Omega_c(3090)} &= 3090.2 \pm 0.3 \pm 0.5 \text{ MeV}, \quad \Gamma_{\Omega_c(3090)} = 8.7 \pm 1.0 \pm 0.8 \text{ MeV}, \\
M_{\Omega_c(3119)} &= 3119.1 \pm 0.3 \pm 0.9 \text{ MeV}, \quad \Gamma_{\Omega_c(3119)} = 1.1 \pm 0.8 \pm 0.4 \text{ MeV}.
\end{aligned} \tag{1}$$

Later, the former four states $\Omega_c(3000)$, $\Omega_c(3050)$, $\Omega_c(3066)$ and $\Omega_c(3090)$ were confirmed by the LHCb and Belle Collaborations [31, 32]. The discovery of the LHCb collaboration has led to a new experimental situation, which requires a more detailed study of heavy baryons and their properties. The discovery of these states, although their quantum numbers have not been determined, could provide new insights into QCD and its complex behavior. This could lead to a deeper understanding of the underlying properties of QCD. However, our information about their properties is still not sufficient and further suggestions for experimental exploration of Ω_c-like states should be addressed. The experimental discoveries were followed by various theoretical studies, investigating them in the conventional baryon, molecular, and compact pentaquark states to shed light on their exact nature and quantum numbers (for details see the Refs. [33–37]).

The literature review indicates that the majority of research has concentrated on computing the spectroscopic and decay parameters of these states. However, it is evident that relying exclusively on spectroscopic and decay

* ulasozdem@aydin.edu.tr

PHILOSOPHICAL TRANSACTIONS A

royalsocietypublishing.org/journal/rsta

Review

Article submitted to journal

Subject Areas:
Astroparticle physics, Neutrino properties, Fundamental particles and interactions

Keywords:
Neutrinos, Gamma rays, Beyond-standard-model physics

Author for correspondence:
Markus Ackermann
e-mail: markus.ackermann@desy.de
Klaus Helbing
e-mail: helbing@uni-wuppertal.de

Searches for beyond-standard-model physics with astroparticle physics instruments

M. Ackermann[1] and K. Helbing[2]

[1]Deutsches Elektronen-Synchrotron DESY, Platanenallee 6, 15738 Zeuthen, Germany
[2]Dept. of Physics, University of Wuppertal, 42119 Wuppertal, Germany

Many instruments for astroparticle physics are primarily geared towards multi-messenger astrophysics, to study the origin of cosmic rays (CR) and to understand high-energy astrophysical processes. Since these instruments observe the Universe at extreme energies and in kinematic ranges not accessible at accelerators these experiments provide also unique and complementary opportunities to search for particles and physics beyond the standard model of particle physics. In particular, the reach of IceCube, Fermi and KATRIN to search for and constrain Dark Matter, Axions, heavy Big Bang relics, sterile neutrinos and Lorentz Invariance Violation (LIV) will be discussed. The contents of this article are based on material presented at the Humboldt-Kolleg "Clues to a mysterious Universe - exploring the interface of particle, gravity and quantum physics" in June 2022.

THE ROYAL SOCIETY PUBLISHING

A direct probe of Λ potential in nuclear medium

Gao-Chan Yong[1,2]
[1] *Institute of Modern Physics, Chinese Academy of Sciences, Lanzhou 730000, China*
[2] *School of Nuclear Science and Technology, University of Chinese Academy of Sciences, Beijing 100049, China*

Using the Liège intranuclear-cascade model together with the ablation model ABLA, an investigation is conducted into the effects of Λ potential in Λ-nucleus and Λ-hypernucleus-nucleus collisions across various beam energies. The findings show that the angle and transverse-momentum distributions of scattered Λ hyperon, the scattering cross section of the Λ hyperon in Λ-nucleus collisions as well as the rapidity distribution of Λ hyperon in Λ-hypernucleus-nucleus collisions are significantly influenced by the strength of the Λ potential in these scattering reactions across various beam energies. These demonstrations, unhindered by the uncertainties of Λ and hypernuclei productions in nuclear medium, allow for a direct investigation of the Λ potential, especially its momentum dependence. The criticality of probing the Λ potential is closely associated with the resolution of the "hyperon puzzle" in neutron stars.

Neutron stars emerge from the ashes of supernova explosions and were initially believed to predominantly consist of neutrons. Nonetheless, a sequence of theoretical studies has suggested that neutron stars might also harbor strange matter [1]. The concept of strangeness in neutron stars could profoundly impact our comprehension of these celestial bodies [2]. This aspect might influence their internal composition and cooling mechanisms, as highlighted in various studies [3–7]. Additionally, the presence of strangeness could alter the dynamics of neutron star mergers [8], potentially leading to distinct gravitational wave signatures [9]. The softening of the equation of state for dense matter, attributed to strangeness, could play a pivotal role in the shock-wave/neutrino-delayed-shock process, thereby affecting the explosive birth of core-collapse supernovae [10–13]. The presence of strangeness within neutron star matter has thus ignited the curiosity of the physics community [14–21], promising to shed light on the strong nuclear force and the characteristics of matter in ultra-extreme conditions, as further explored in references [19, 21–24]. Consequently, the study of hyperon-nucleon interactions and the significance of strangeness in neutron stars arises as a vital domain for astrophysicists, together with particle and nuclear physicists.

The resolution of the "hyperon puzzle", focusing on the inclusion of strangeness within the nuclear medium to ascertain the strong nuclear force, remains a fundamental query [22]. A variety of theoretical approaches have been adopted, such as utilizing nuclear many-body theories for calculating the properties of strange particles in dense environments [18, 24], applying effective field theories to elucidate the interactions between strange particles and nucleons [25], using perturbative quantum chromodynamics for the study of strange quark matter [26, 27]. Astrophysical observations of neutron stars also serve as a means to deduce the characteristics of strange particles within [28, 29].

Despite these methodologies, interactions between strangeness and non-strangeness in nuclear matter confront considerable theoretical ambiguities and are seldom directly examined through nuclear experiments in terrestrial labs. In Ref. [30], it is argued that combining studies of transport models with nuclear experimental data from facilities around the world could be a better way to address the "hyperon puzzle". Therefore, nuclear reactions may offer a more effective method for studying hyperon-nucleon interactions within nuclear medium: Hyperon-nucleus scattering experiments deal with hyperon-nucleon interactions in medium around saturation density, whereas hypernucleus-nucleus collisions examine these interactions at higher densities. By adjusting the beam energy, one can also explore the momentum dependence of hyperon-nucleon interactions in nuclear medium. In this study, the Liège intranuclear-cascade (INCL) model, combined with the ABLA deexcitation code, is employed to investigate the effects of the Λ potential around and above normal nuclear density. It's demonstrated that experiments involving Λ-nucleus and hypernucleus-nucleus collisions could directly unveil the Λ-nucleon interactions in nuclear medium.

The Liège intranuclear-cascade code, also known as the INCL model [31–33], is used to describe the collision between a projectile (such as nucleons, pions, hyperons and light ions) and a target nucleus. The INCL model incorporates classical physics principles, but also includes some quantum-mechanical features (such as Fermi motion, realistic space densities and Pauli blocking) to account for the initial conditions and dynamics of the collision. The INCL model treats an energy and isospin-dependent nucleon potential and an isospin-dependent constant hyperon potential with Woods-Saxon density distributions [32, 34, 35]. The model treats nuclear collisions as successive relativistic binary hadron-hadron collisions, where the positions and momenta of the hadrons are tracked over time. The extended INCL model includes the production of pion mesons and strange particles [36, 37]. The latest version of the model, INCL++6.32, includes the formation of hyperremnants [38, 39]. Based on different kinds of conservation laws (such as for baryon number, charge, energy, momentum, and angular momentum), the model predicts the formation of hot hyperremnants and characterizes them in terms of atomic and mass numbers, strangeness number,

Nikhef-2023-020
TIF-UNIMI-2023-23
Edinburgh 2023/29

The Path to N^{3}LO Parton Distributions

The NNPDF Collaboration:
Richard D. Ball[1], Andrea Barontini[2], Alessandro Candido[2,3], Stefano Carrazza[2], Juan Cruz-Martinez[3], Luigi Del Debbio[1], Stefano Forte[2], Tommaso Giani[4,5], Felix Hekhorn[2,6,7], Zahari Kassabov[8], Niccolò Laurenti,[2] Giacomo Magni[4,5], Emanuele R. Nocera[9], Tanjona R. Rabemananjara[4,5], Juan Rojo[4,5], Christopher Schwan[10], Roy Stegeman[1], and Maria Ubiali[8]

[1] *The Higgs Centre for Theoretical Physics, University of Edinburgh, JCMB, KB, Mayfield Rd, Edinburgh EH9 3JZ, Scotland*
[2] *Tif Lab, Dipartimento di Fisica, Università di Milano and INFN, Sezione di Milano, Via Celoria 16, I-20133 Milano, Italy*
[3] *CERN, Theoretical Physics Department, CH-1211 Geneva 23, Switzerland*
[4] *Department of Physics and Astronomy, Vrije Universiteit, NL-1081 HV Amsterdam*
[5] *Nikhef Theory Group, Science Park 105, 1098 XG Amsterdam, The Netherlands*
[6] *University of Jyvaskyla, Department of Physics, P.O. Box 35, FI-40014 University of Jyvaskyla, Finland*
[7] *Helsinki Institute of Physics, P.O. Box 64, FI-00014 University of Helsinki, Finland*
[8] *DAMTP, University of Cambridge, Wilberforce Road, Cambridge, CB3 0WA, United Kingdom*
[9] *Dipartimento di Fisica, Università degli Studi di Torino and INFN, Sezione di Torino, Via Pietro Giuria 1, I-10125 Torino, Italy*
[10] *Universität Würzburg, Institut für Theoretische Physik und Astrophysik, 97074 Würzburg, Germany*

This paper is dedicated to the memory of Stefano Catani, Grand Master of QCD, great scientist and human being

Abstract

We extend the existing leading (LO), next-to-leading (NLO), and next-to-next-to-leading order (NNLO) NNPDF4.0 sets of parton distribution functions (PDFs) to approximate next-to-next-to-next-to-leading order (aN^{3}LO). We construct an approximation to the N^{3}LO splitting functions that includes all available partial information from both fixed-order computations and from small and large x resummation, and estimate the uncertainty on this approximation by varying the set of basis functions used to construct the approximation. We include known N^{3}LO corrections to deep-inelastic scattering structure functions and extend the FONLL general-mass scheme to $\mathcal{O}\left(\alpha_s^3\right)$ accuracy. We determine a set of aN^{3}LO PDFs by accounting both for the uncertainty on splitting functions due to the incomplete knowledge of N^{3}LO terms, and to the uncertainty related to missing higher corrections (MHOU), estimated by scale variation, through a theory covariance matrix formalism. We assess the perturbative stability of the resulting PDFs, we study the impact of MHOUs on them, and we compare our results to the aN^{3}LO PDFs from the MSHT group. We examine the phenomenological impact of aN^{3}LO corrections on parton luminosities at the LHC, and give a first assessment of the impact of aN^{3}LO PDFs on the Higgs and Drell-Yan total production cross-sections. We find that the aN^{3}LO NNPDF4.0 PDFs are consistent within uncertainties with their NNLO counterparts, that they improve the description of the global dataset and the perturbative convergence of Higgs and Drell-Yan cross-sections, and that MHOUs on PDFs decrease substantially with the increase of perturbative order.

New Pathways in Neutrino Physics via Quantum-Encoded Data Analysis

Jeffrey Lazar*
Department of Physics and Wisconsin IceCube Particle Astrophysics Center, University of Wisconsin–Madison, Madison, WI 53706, USA and Department of Physics and Laboratory for Particle Physics and Cosmology, Harvard University, Cambridge, MA 02138, US

Santiago Giner Olavarrieta† and Carlos A. Argüelles‡
Department of Physics and Laboratory for Particle Physics and Cosmology, Harvard University, Cambridge, MA 02138, US

Giancarlo Gatti§
Department of Physical Chemistry, University of the Basque Country UPV/EHU, Apartado 644, 48080 Bilbao, Spain EHU Quantum Center, University of the Basque Country UPV/EHU, Apartado 644, 48080 Bilbao, Spain and Quantum Mads, Uribitarte Kalea 6, 48001 Bilbao, Spain

Mikel Sanz¶
Department of Physical Chemistry, University of the Basque Country UPV/EHU, Apartado 644, 48080 Bilbao, Spain EHU Quantum Center, University of the Basque Country UPV/EHU, Apartado 644, 48080 Bilbao, Spain IKERBASQUE, Basque Foundation for Science, Plaza Euskadi 5, 48009, Bilbao, Spain and Basque Center for Applied Mathematics (BCAM), Alameda de Mazarredo, 14, 48009 Bilbao, Spain

Ever-increasing amount of data is produced by particle detectors in their quest to unveil the laws of Nature. The large data rate requires the use of specialized triggers that promptly reduce the data rate to a manageable level; however, in doing so, unexpected new phenomena may escape detection. Additionally, the large data rate is increasingly difficult to analyze effectively, which has led to a recent revolution on machine learning techniques. Here, we present a methodology based on recent quantum compression techniques that has the capacity to store exponentially more amount of information than classically available methods. To demonstrate this, we encode the full neutrino telescope event information using parity observables in an IBM quantum processor using 8 qubits. Then we show that we can recover the information stored on the quantum computer with a fidelity of 84%. Finally, we illustrate the use of our protocol by performing a classification task that separates electron-neutrino events to muon-neutrinos events in a neutrino telescope. This new capability would eventually allow us to solve the street light effect in particle physics, where we only record signatures of particles with which we are familiar.

Since the Geiger-Muller counter was used to trigger on α particles in 1928, automated triggering systems have become increasingly important to experimental high-energy physics [1]. The increased need for higher intensity and higher energy beams resulted in the development of faster electronics and complementary data storage and analysis techniques. In particular, the development of magnetic storage on tapes, disks, and solid state drives (see Fig. 1 (A)) enabled the *Big Data* paradigm of particle physics, culminating in the 2012 discovery of the Higgs Boson at the Large Hadron Collider (LHC) [2, 3]. The lockstep development of the Standard Model (SM) and novel data storage techniques echoes the historical precedent, where efficient data storage and retrieval has been central to advancing our understanding of Nature.

While the successes of our current paradigm are undeniable [4], significant questions remain unanswered on both the largest and the smallest scales. For example, on galactic and cosmological scales, the SM cannot provide a viable dark matter candidate. Furthermore, at the sub-nuclear scale, the origin and smallness of neutrino masses continue to elude us. In an attempt to answer these questions, high-energy physics (HEP) experiments use triggers inspired by familiar physics models to select and reduce the data to a manageable level; however, this approach leaves us vulnerable to the so-called streetlight effect, an observational bias which leads us to only search in the best known areas. As we continue to pursue new physics, we may need to relax these filters to allow in previously unconsidered types of events.

This need to expand our searches to new regions is happening against the backdrop of a crisis of data management and acquisition in HEP. For example, every day, the IceCube Neutrino Observatory produces one Terabyte (TB) of data [5], while the LHC produces nearly 300 TB in the same period [6]. Additionally, both experiments have planned upgrades [7, 8] that will increase their data production by an order of magnitude, IceCube by expanding its volume and the LHC by increasing its luminosity. Beyond these two experiments, many other large volume next-generation experiments such as DUNE [9] and HyperKamiokande [10] are expected to face similar challenges. While it may be possible to meet these data needs using current technologies, selecting and storing large fractions of the data will become increasingly untenable, rendering us more vulnerable to the streetlight

First simultaneous measurement of differential muon-neutrino charged-current cross sections on argon for final states with and without protons using MicroBooNE data

P. Abratenko,[38] O. Alterkait,[38] D. Andrade Aldana,[15] L. Arellano,[21] J. Asaadi,[37] A. Ashkenazi,[35] S. Balasubramanian,[12] B. Baller,[12] G. Barr,[28] D. Barrow,[28] J. Barrow,[22,25,35] V. Basque,[12] O. Benevides Rodrigues,[15] S. Berkman,[12,24] A. Bhanderi,[21] A. Bhat,[7] M. Bhattacharya,[12] M. Bishai,[3] A. Blake,[18] B. Bogart,[23] T. Bolton,[17] J. Y. Book,[14] M. B. Brunetti,[41] L. Camilleri,[10] Y. Cao,[21] D. Caratelli,[4] F. Cavanna,[12] G. Cerati,[12] A. Chappell,[41] Y. Chen,[31] J. M. Conrad,[22] M. Convery,[31] L. Cooper-Troendle,[29] J. I. Crespo-Anadón,[6] R. Cross,[41] M. Del Tutto,[12] S. R. Dennis,[5] P. Detje,[5] A. Devitt,[18] R. Diurba,[2] Z. Djurcic,[1] R. Dorrill,[15] K. Duffy,[28] S. Dytman,[29] B. Eberly,[33] P. Englezos,[30] A. Ereditato,[7,12] J. J. Evans,[21] R. Fine,[19] O. G. Finnerud,[21] W. Foreman,[15] B. T. Fleming,[7] D. Franco,[7] A. P. Furmanski,[25] F. Gao,[4] D. Garcia-Gamez,[13] S. Gardiner,[12] G. Ge,[10] S. Gollapinni,[19] E. Gramellini,[21] P. Green,[28] H. Greenlee,[12] L. Gu,[18] W. Gu,[3] R. Guenette,[21] P. Guzowski,[21] L. Hagaman,[7] O. Hen,[22] C. Hilgenberg,[25] G. A. Horton-Smith,[17] Z. Imani,[38] B. Irwin,[25] M. S. Ismail,[29] C. James,[12] X. Ji,[26] J. H. Jo,[3] R. A. Johnson,[8] Y.-J. Jwa,[10] D. Kalra,[10] N. Kamp,[22] G. Karagiorgi,[10] W. Ketchum,[12] M. Kirby,[3,12] T. Kobilarcik,[12] I. Kreslo,[2] M. B. Leibovitch,[4] I. Lepetic,[30] J.-Y. Li,[11] K. Li,[42] Y. Li,[3] K. Lin,[30] B. R. Littlejohn,[15] H. Liu,[3] W. C. Louis,[19] X. Luo,[4] C. Mariani,[40] D. Marsden,[21] J. Marshall,[41] N. Martinez,[17] D. A. Martinez Caicedo,[32] S. Martynenko,[3] A. Mastbaum,[30] I. Mawby,[18] N. McConkey,[39] V. Meddage,[17] J. Micallef,[22,38] K. Miller,[7] A. Mogan,[9] T. Mohayai,[12,16] M. Mooney,[9] A. F. Moor,[5] C. D. Moore,[12] L. Mora Lepin,[21] M. M. Moudgalya,[21] S. Mulleriababu,[2] D. Naples,[29] A. Navrer-Agasson,[21] N. Nayak,[3] M. Nebot-Guinot,[11] J. Nowak,[18] N. Oza,[10] O. Palamara,[12] N. Pallat,[25] V. Paolone,[29] A. Papadopoulou,[1] V. Papavassiliou,[27] H. B. Parkinson,[11] S. F. Pate,[27] N. Patel,[18] Z. Pavlovic,[12] E. Piasetzky,[35] I. Pophale,[18] X. Qian,[3] J. L. Raaf,[12] V. Radeka,[3] A. Rafique,[1] M. Reggiani-Guzzo,[11,21] L. Ren,[27] L. Rochester,[31] J. Rodriguez Rondon,[32] M. Rosenberg,[38] M. Ross-Lonergan,[19] C. Rudolf von Rohr,[2] I. Safa,[10] G. Scanavini,[42] D. W. Schmitz,[7] A. Schukraft,[12] W. Seligman,[10] M. H. Shaevitz,[10] R. Sharankova,[12] J. Shi,[5] E. L. Snider,[12] M. Soderberg,[34] S. Söldner-Rembold,[21] J. Spitz,[23] M. Stancari,[12] J. St. John,[12] T. Strauss,[12] A. M. Szelc,[11] W. Tang,[36] N. Taniuchi,[5] K. Terao,[31] C. Thorpe,[18,21] D. Torbunov,[3] D. Totani,[4] M. Toups,[12] Y.-T. Tsai,[31] J. Tyler,[17] M. A. Uchida,[5] T. Usher,[31] B. Viren,[3] M. Weber,[2] H. Wei,[20] A. J. White,[7] S. Wolbers,[12] T. Wongjirad,[38] M. Wospakrik,[12] K. Wresilo,[5] W. Wu,[12,29] E. Yandel,[4] T. Yang,[12] L. E. Yates,[12] H. W. Yu,[3] G. P. Zeller,[12] J. Zennamo,[12] and C. Zhang[3]

(The MicroBooNE Collaboration)*

[1] *Argonne National Laboratory (ANL), Lemont, IL, 60439, USA*
[2] *Universität Bern, Bern CH-3012, Switzerland*
[3] *Brookhaven National Laboratory (BNL), Upton, NY, 11973, USA*
[4] *University of California, Santa Barbara, CA, 93106, USA*
[5] *University of Cambridge, Cambridge CB3 0HE, United Kingdom*
[6] *Centro de Investigaciones Energéticas, Medioambientales y Tecnológicas (CIEMAT), Madrid E-28040, Spain*
[7] *University of Chicago, Chicago, IL, 60637, USA*
[8] *University of Cincinnati, Cincinnati, OH, 45221, USA*
[9] *Colorado State University, Fort Collins, CO, 80523, USA*
[10] *Columbia University, New York, NY, 10027, USA*
[11] *University of Edinburgh, Edinburgh EH9 3FD, United Kingdom*
[12] *Fermi National Accelerator Laboratory (FNAL), Batavia, IL 60510, USA*
[13] *Universidad de Granada, Granada E-18071, Spain*
[14] *Harvard University, Cambridge, MA 02138, USA*
[15] *Illinois Institute of Technology (IIT), Chicago, IL 60616, USA*
[16] *Indiana University, Bloomington, IN 47405, USA*
[17] *Kansas State University (KSU), Manhattan, KS, 66506, USA*
[18] *Lancaster University, Lancaster LA1 4YW, United Kingdom*
[19] *Los Alamos National Laboratory (LANL), Los Alamos, NM, 87545, USA*
[20] *Louisiana State University, Baton Rouge, LA, 70803, USA*
[21] *The University of Manchester, Manchester M13 9PL, United Kingdom*
[22] *Massachusetts Institute of Technology (MIT), Cambridge, MA, 02139, USA*
[23] *University of Michigan, Ann Arbor, MI, 48109, USA*
[24] *Michigan State University, East Lansing, MI 48824, USA*
[25] *University of Minnesota, Minneapolis, MN, 55455, USA*
[26] *Nankai University, Nankai District, Tianjin 300071, China*

[27] *New Mexico State University (NMSU), Las Cruces, NM, 88003, USA*
[28] *University of Oxford, Oxford OX1 3RH, United Kingdom*
[29] *University of Pittsburgh, Pittsburgh, PA, 15260, USA*
[30] *Rutgers University, Piscataway, NJ, 08854, USA*
[31] *SLAC National Accelerator Laboratory, Menlo Park, CA, 94025, USA*
[32] *South Dakota School of Mines and Technology (SDSMT), Rapid City, SD, 57701, USA*
[33] *University of Southern Maine, Portland, ME, 04104, USA*
[34] *Syracuse University, Syracuse, NY, 13244, USA*
[35] *Tel Aviv University, Tel Aviv, Israel, 69978*
[36] *University of Tennessee, Knoxville, TN, 37996, USA*
[37] *University of Texas, Arlington, TX, 76019, USA*
[38] *Tufts University, Medford, MA, 02155, USA*
[39] *University College London, London WC1E 6BT, United Kingdom*
[40] *Center for Neutrino Physics, Virginia Tech, Blacksburg, VA, 24061, USA*
[41] *University of Warwick, Coventry CV4 7AL, United Kingdom*
[42] *Wright Laboratory, Department of Physics, Yale University, New Haven, CT, 06520, USA*

(Dated: February 29 2024)

We report the first double-differential neutrino-argon cross section measurement made simultaneously for final states with and without protons for the inclusive muon neutrino charged-current interaction channel. The proton kinematics of this channel are further explored with a differential cross section measurement as a function of the leading proton's kinetic energy that extends across the detection threshold. These measurements utilize data collected using the MicroBooNE detector from $6.4{\times}10^{20}$ protons on target from the Fermilab Booster Neutrino Beam with a mean neutrino energy of ∼0.8 GeV. Extensive data-driven model validation utilizing the conditional constraint formalism is employed. This motivates enlarging the uncertainties with an empirical reweighting approach to minimize the possibility of extracting biased cross section results. The extracted nominal flux-averaged cross sections are compared to widely used event generator predictions revealing severe mismodeling of final states without protons for muon neutrino charged-current interactions, possibly from insufficient treatment of final state interactions. These measurements provide a wealth of new information useful for improving event generators which will enhance the sensitivity of precision measurements in neutrino experiments.

Neutrino experiments measure flavor oscillations as a function of neutrino energy in order to determine neutrino mixing parameters and search for new physics beyond the Standard Model [1–5]. This requires precise mapping between reconstructed and true neutrino energy. The inclusive muon neutrino charged current (ν_μCC) interaction channel, $\nu_\mu \mathrm{N} \to \mu^- X$, where N is the struck nucleus and X is the hadronic final state, is important for these measurements because it identifies the neutrino flavor with high purity and efficiency due to the sole requirement of detecting the muon.

A number of these neutrino experiments utilize liquid argon time projection chambers (LArTPCs) [5, 6]. These tracking calorimeters have low detection thresholds and excellent particle identification (PID) capabilities [7–11]. LArTPCs enable the inclusive ν_μCC channel to be divided into subchannels based on the composition of the final state, each having a different mapping between true and reconstructed neutrino energy. This improves the energy reconstruction and increases the sensitivity of precision measurements [12].

Maximizing the physics reach of LArTPCs requires neutrino-argon interaction modeling capable of describing all final state particles. Existing models are unable to describe data with such detail, necessitating large interaction modeling uncertainties [12, 13]. This is unsurprising; theoretical models attempting to describe experimental observables must simultaneously account for multiple scattering mechanisms [14], in-medium nuclear modifications to the fundamental neutrino interactions [15, 16], and final-state interactions (FSI) involving the hadronic reaction products as they exit the nucleus [17]. The prominence of nuclear effects grows with the size of the target nucleus, further complicating the modeling of scattering for heavy nuclei like argon.

Efforts to simulate ν_μCC interactions benefit from measurements that simultaneously probe the leptonic and hadronic kinematics. Building on previous MicroBooNE work [18–20], we report a double-differential measurement of the muon energy, E_μ, and muon scattering angle with respect to the neutrino beam, $\cos\theta_\mu$, for the ν_μCC channel split into final states with one or more protons ("Np" where N≥ 1) and without protons ("0p"). An event is only included in the Np signal if the leading proton exiting the nucleus has kinetic energy above 35 MeV, which roughly corresponds to the proton tracking threshold in MicroBooNE [21]. The proton kinematics are further explored with a differential cross section measurement of the inclusive ν_μCC channel ("Xp" where

* microboone_info@fnal.gov

Inclusive cross section measurements in final states with and without protons for charged-current ν_μ-Ar scattering in MicroBooNE

P. Abratenko,[38] O. Alterkait,[38] D. Andrade Aldana,[15] L. Arellano,[21] J. Asaadi,[37] A. Ashkenazi,[35] S. Balasubramanian,[12] B. Baller,[12] G. Barr,[28] D. Barrow,[28] J. Barrow,[22,25,35] V. Basque,[12] O. Benevides Rodrigues,[15] S. Berkman,[12,24] A. Bhanderi,[21] A. Bhat,[7] M. Bhattacharya,[12] M. Bishai,[3] A. Blake,[18] B. Bogart,[23] T. Bolton,[17] J. Y. Book,[14] M. B. Brunetti,[41] L. Camilleri,[10] Y. Cao,[21] D. Caratelli,[4] F. Cavanna,[12] G. Cerati,[12] A. Chappell,[41] Y. Chen,[31] J. M. Conrad,[22] M. Convery,[31] L. Cooper-Troendle,[29] J. I. Crespo-Anadón,[6] R. Cross,[41] M. Del Tutto,[12] S. R. Dennis,[5] P. Detje,[5] A. Devitt,[18] R. Diurba,[2] Z. Djurcic,[1] R. Dorrill,[15] K. Duffy,[28] S. Dytman,[29] B. Eberly,[33] P. Englezos,[30] A. Ereditato,[7,12] J. J. Evans,[21] R. Fine,[19] O. G. Finnerud,[21] W. Foreman,[15] B. T. Fleming,[7] D. Franco,[7] A. P. Furmanski,[25] F. Gao,[4] D. Garcia-Gamez,[13] S. Gardiner,[12] G. Ge,[10] S. Gollapinni,[19] E. Gramellini,[21] P. Green,[28] H. Greenlee,[12] L. Gu,[18] W. Gu,[3] R. Guenette,[21] P. Guzowski,[21] L. Hagaman,[7] O. Hen,[22] C. Hilgenberg,[25] G. A. Horton-Smith,[17] Z. Imani,[38] B. Irwin,[25] M. S. Ismail,[29] C. James,[12] X. Ji,[26] J. H. Jo,[3] R. A. Johnson,[8] Y.-J. Jwa,[10] D. Kalra,[10] N. Kamp,[22] G. Karagiorgi,[10] W. Ketchum,[12] M. Kirby,[3,12] T. Kobilarcik,[12] I. Kreslo,[2] M. B. Leibovitch,[4] I. Lepetic,[30] J.-Y. Li,[11] K. Li,[42] Y. Li,[3] K. Lin,[30] B. R. Littlejohn,[15] H. Liu,[3] W. C. Louis,[19] X. Luo,[4] C. Mariani,[40] D. Marsden,[21] J. Marshall,[41] N. Martinez,[17] D. A. Martinez Caicedo,[32] S. Martynenko,[3] A. Mastbaum,[30] I. Mawby,[18] N. McConkey,[39] V. Meddage,[17] J. Micallef,[22,38] K. Miller,[7] A. Mogan,[9] T. Mohayai,[12,16] M. Mooney,[9] A. F. Moor,[5] C. D. Moore,[12] L. Mora Lepin,[21] M. M. Moudgalya,[21] S. Mulleriababu,[2] D. Naples,[29] A. Navrer-Agasson,[21] N. Nayak,[3] M. Nebot-Guinot,[11] J. Nowak,[18] N. Oza,[10] O. Palamara,[12] N. Pallat,[25] V. Paolone,[29] A. Papadopoulou,[1] V. Papavassiliou,[27] H. B. Parkinson,[11] S. F. Pate,[27] N. Patel,[18] Z. Pavlovic,[12] A. Pellot Jimenez,[23] E. Piasetzky,[35] I. Pophale,[18] X. Qian,[3] J. L. Raaf,[12] V. Radeka,[3] A. Rafique,[1] M. Reggiani-Guzzo,[11,21] L. Ren,[27] L. Rochester,[31] J. Rodriguez Rondon,[32] M. Rosenberg,[38] M. Ross-Lonergan,[19] C. Rudolf von Rohr,[2] I. Safa,[10] G. Scanavini,[42] D. W. Schmitz,[7] A. Schukraft,[12] W. Seligman,[10] M. H. Shaevitz,[10] R. Sharankova,[12] J. Shi,[5] E. L. Snider,[12] M. Soderberg,[34] S. Söldner-Rembold,[21] J. Spitz,[23] M. Stancari,[12] J. St. John,[12] T. Strauss,[12] A. M. Szelc,[11] W. Tang,[36] N. Taniuchi,[5] K. Terao,[31] C. Thorpe,[18,21] D. Torbunov,[3] D. Totani,[4] M. Toups,[12] Y.-T. Tsai,[31] J. Tyler,[17] M. A. Uchida,[5] T. Usher,[31] B. Viren,[3] M. Weber,[2] H. Wei,[20] A. J. White,[7] S. Wolbers,[12] T. Wongjirad,[38] M. Wospakrik,[12] K. Wresilo,[5] W. Wu,[12,29] E. Yandel,[4] T. Yang,[12] L. E. Yates,[12] H. W. Yu,[3] G. P. Zeller,[12] J. Zennamo,[12] and C. Zhang[3]

(The MicroBooNE Collaboration)*

[1] *Argonne National Laboratory (ANL), Lemont, IL, 60439, USA*
[2] *Universität Bern, Bern CH-3012, Switzerland*
[3] *Brookhaven National Laboratory (BNL), Upton, NY, 11973, USA*
[4] *University of California, Santa Barbara, CA, 93106, USA*
[5] *University of Cambridge, Cambridge CB3 0HE, United Kingdom*
[6] *Centro de Investigaciones Energéticas, Medioambientales y Tecnológicas (CIEMAT), Madrid E-28040, Spain*
[7] *University of Chicago, Chicago, IL, 60637, USA*
[8] *University of Cincinnati, Cincinnati, OH, 45221, USA*
[9] *Colorado State University, Fort Collins, CO, 80523, USA*
[10] *Columbia University, New York, NY, 10027, USA*
[11] *University of Edinburgh, Edinburgh EH9 3FD, United Kingdom*
[12] *Fermi National Accelerator Laboratory (FNAL), Batavia, IL 60510, USA*
[13] *Universidad de Granada, Granada E-18071, Spain*
[14] *Harvard University, Cambridge, MA 02138, USA*
[15] *Illinois Institute of Technology (IIT), Chicago, IL 60616, USA*
[16] *Indiana University, Bloomington, IN 47405, USA*
[17] *Kansas State University (KSU), Manhattan, KS, 66506, USA*
[18] *Lancaster University, Lancaster LA1 4YW, United Kingdom*
[19] *Los Alamos National Laboratory (LANL), Los Alamos, NM, 87545, USA*
[20] *Louisiana State University, Baton Rouge, LA, 70803, USA*
[21] *The University of Manchester, Manchester M13 9PL, United Kingdom*
[22] *Massachusetts Institute of Technology (MIT), Cambridge, MA, 02139, USA*
[23] *University of Michigan, Ann Arbor, MI, 48109, USA*
[24] *Michigan State University, East Lansing, MI 48824, USA*
[25] *University of Minnesota, Minneapolis, MN, 55455, USA*
[26] *Nankai University, Nankai District, Tianjin 300071, China*
[27] *New Mexico State University (NMSU), Las Cruces, NM, 88003, USA*
[28] *University of Oxford, Oxford OX1 3RH, United Kingdom*

[29] *University of Pittsburgh, Pittsburgh, PA, 15260, USA*
[30] *Rutgers University, Piscataway, NJ, 08854, USA*
[31] *SLAC National Accelerator Laboratory, Menlo Park, CA, 94025, USA*
[32] *South Dakota School of Mines and Technology (SDSMT), Rapid City, SD, 57701, USA*
[33] *University of Southern Maine, Portland, ME, 04104, USA*
[34] *Syracuse University, Syracuse, NY, 13244, USA*
[35] *Tel Aviv University, Tel Aviv, Israel, 69978*
[36] *University of Tennessee, Knoxville, TN, 37996, USA*
[37] *University of Texas, Arlington, TX, 76019, USA*
[38] *Tufts University, Medford, MA, 02155, USA*
[39] *University College London, London WC1E 6BT, United Kingdom*
[40] *Center for Neutrino Physics, Virginia Tech, Blacksburg, VA, 24061, USA*
[41] *University of Warwick, Coventry CV4 7AL, United Kingdom*
[42] *Wright Laboratory, Department of Physics, Yale University, New Haven, CT, 06520, USA*

(Dated: February 29 2024)

A detailed understanding of inclusive muon neutrino charged-current interactions on argon is crucial to the study of neutrino oscillations in current and future experiments using liquid argon time projection chambers. To that end, we report a comprehensive set of differential cross section measurements for this channel that simultaneously probe the leptonic and hadronic systems by dividing the channel into final states with and without protons. Measurements of the proton kinematics and proton multiplicity of the final state are also presented. For these measurements, we utilize data collected with the MicroBooNE detector from 6.4×10^{20} protons on target from the Fermilab Booster Neutrino Beam at a mean neutrino energy of approximately 0.8 GeV. We present in detail the cross section extraction procedure, including the unfolding, and model validation that uses data to model comparisons and the conditional constraint formalism to detect mismodeling that may introduce biases to extracted cross sections that are larger than their uncertainties. The validation exposes insufficiencies in the overall model, motivating the inclusion of an additional data-driven reweighting systematic to ensure the accuracy of the unfolding. The extracted results are compared to a number of event generators and their performance is discussed with a focus on the regions of phase-space that indicate the greatest need for modeling improvements.

I. INTRODUCTION

A detailed understanding of inclusive muon neutrino charged-current interactions (ν_μCC) on argon is necessary to perform precision measurements of neutrino oscillations and search for new physics beyond the Standard Model in current and future accelerator-based experiments using liquid argon time projection chambers (LArTPCs) [1, 2]. These experiments, which measure flavor oscillation as a function of neutrino energy, will address several important topics in neutrino physics including: charge-parity violation in the neutrino sector [3, 4], the neutrino mass ordering [5], and sterile neutrinos [6]. As such, the ability to accurately identify neutrino flavor and measure the neutrino energy, E_ν, is essential. With only the requirement of detecting the charged muon in the final state, the inclusive ν_μCC channel is able to identify muon neutrino flavor with high efficiency and purity. While the energy, E_μ, and scattering angle, θ_μ, of the outgoing muon can be directly measured, the use of broad-band neutrino beams means E_ν is not known apriori on an event-by-event basis and can only be deduced by measuring the hadronic energy of the final state particles. Thus, an accurate mapping from the true to reconstructed neutrino energy is needed in order to maximize the physics reach of accelerator-based neutrino experiments.

Mapping from reconstructed to true E_ν is complicated by the fact that, because E_ν is not known on an event by event basis, approximate separation of interaction modes cannot be achieved as easily as in narrow-band electron beam experiments [7]. Theoretical models attempting to describe experimental observables must therefore simultaneously account for multiple scattering mechanisms. For experiments using a target with a heavy nucleus, various nuclear effects [8], including nuclear ground state modeling, nucleon-nucleon correlations, and final state interactions (FSI), introduce additional challenges to the model of the complete final state. Existing models and the event generators that employ them are unable to describe data with such detail, necessitating large cross section modeling uncertainties [9, 10]. This creates a need for a diverse set of detailed neutrino-nucleus cross section measurements that can benchmark refinements to models and event generators. Such measurements will stimulate the improvement of theoretical modeling, which can help improve the sensitivity of future neutrino experiments in a variety of ways [9, 11].

In the past decades, there have been continuous advancements in measuring cross sections of inclusive and exclusive neutrino-nucleus interactions ([12–15] for example). In particular, triple-differential cross sections as a function of muon kinematics and total observed hadronic

* microboone_info@fnal.gov

EUROPEAN ORGANISATION FOR NUCLEAR RESEARCH (CERN)

Submitted to: Phys. Lett. B.

CERN-EP-2024-037
1st March 2024

Searches for exclusive Higgs boson decays into $D^*\gamma$ and Z boson decays into $D^0\gamma$ and $K^0_s\gamma$ in pp collisions at $\sqrt{s} = 13$ TeV with the ATLAS detector

The ATLAS Collaboration

Searches for exclusive decays of the Higgs boson into $D^*\gamma$ and of the Z boson into $D^0\gamma$ and $K^0_s\gamma$ can probe flavour-violating Higgs boson and Z boson couplings to light quarks. Searches for these decays are performed with a pp collision data sample corresponding to an integrated luminosity of 136.3 fb^{-1} collected at $\sqrt{s} = 13$ TeV between 2016–2018 with the ATLAS detector at the CERN Large Hadron Collider. In the $D^*\gamma$ and $D^0\gamma$ channels, the observed (expected) 95% confidence-level upper limits on the respective branching fractions are $\mathcal{B}(H \to D^*\gamma) < 1.0(1.2) \times 10^{-3}$, $\mathcal{B}(Z \to D^0\gamma) < 4.0(3.4) \times 10^{-6}$, while the corresponding results in the $K^0_s\gamma$ channel are $\mathcal{B}(Z \to K^0_s\gamma) < 3.1(3.0) \times 10^{-6}$.

1 Introduction

After the observation of the Higgs boson (H) with a mass of 125 GeV by the ATLAS [1] and CMS [2] Collaborations [3, 4], many studies were performed to measure its properties which, so far, are consistent with the Standard Model (SM) expectations [5, 6]. These have confirmed its role in the spontaneous breaking of electroweak symmetry and the mass generation of the massive vector bosons [7, 8]. A complete observation of the Higgs boson Yukawa couplings to third-generation charged fermions was achieved by the ATLAS and CMS collaborations through the observation of the decays $H \to \tau^+\tau^-$ [9, 10] and $H \to b\bar{b}$ [11, 12], and the production of Higgs bosons with top-quark pairs [13, 14]. Evidence was also reported for the decay $H \to \mu^+\mu^-$ [15, 16], and direct searches for $H \to c\bar{c}$ [17, 18] and $H \to e^+e^-$ decays [19, 20] were made, but there is no further experimental evidence for the Higgs boson couplings to the first and second generations of fermions. Instead, the light (u, d, s) quark couplings to the Higgs boson are loosely constrained by existing data on the total Higgs boson's width and combined measurements of Higgs boson production and decays [5, 6].

The ATLAS and CMS Collaborations have also investigated potential beyond-the-SM (BSM) couplings of the Higgs boson, including searches for the lepton-flavour-violating decays $H \to e\mu$, $H \to e\tau$ and $H \to \mu\tau$ [19, 21–23] and for flavour-changing neutral currents via the t-quark decays $t \to cH$ and $t \to uH$ [24–27]. An overview of BSM theories which allow flavour-violating couplings of the Higgs boson to quarks is presented in Ref. [28]. These include BSM scenarios such as the minimal flavour violation framework [29] and the Giudice–Lebedev Higgs boson dependent Yukawa couplings model [30].

Rare exclusive decays of the Higgs boson into a meson and a photon probe both the potential flavour-violating Higgs boson couplings and the Yukawa couplings of the SM [31–38]. Analogous decays of the Z boson into a meson and a photon offer unique tests of the factorisation approach in quantum chromodynamics, QCD [39–41], and in particular, probes of potential flavour-changing neutral current interactions of the Z boson via such decays are discussed in Ref. [40]. Searches for these exclusive decays were made by the ATLAS and CMS Collaborations [42–49], and the ATLAS constraints on them, with corresponding SM predictions, are summarised in Ref. [50]. Figure 1 shows an illustrative Feynman diagram of the $H(Z) \to \mathcal{M}\gamma$ process (where $\mathcal{M}$ denotes a meson) which proceeds via a flavour-violating coupling that can be probed with searches for exclusive Higgs bosons and Z boson decays into a meson and a photon, as done previously in the ATLAS search for $H \to K^*\gamma$ [47].

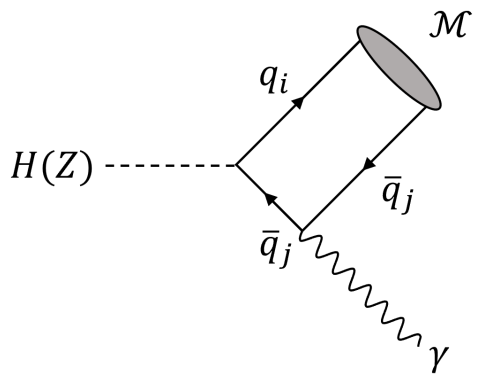

Figure 1: An illustrative Feynman diagram depicting the flavour-violating $H \to \mathcal{M}\gamma$ and $Z \to \mathcal{M}\gamma$ processes considered in this search, where $\mathcal{M}$ is a flavoured meson. For Higgs boson decays, $\mathcal{M} = D^*$; for Z boson decays, $\mathcal{M} = D^0, K^0_s$. The indices i and j refer to the flavour of the quark, and $i \neq j$.

EUROPEAN ORGANIZATION FOR NUCLEAR RESEARCH (CERN)

CERN-EP-2024-022
2024/03/01

CMS-EXO-22-017

Search for long-lived heavy neutral leptons decaying in the CMS muon detectors in proton-proton collisions at $\sqrt{s} = 13\,\text{TeV}$

The CMS Collaboration*

Abstract

A search for heavy neutral leptons (HNLs) decaying in the CMS muon system is presented. A data sample is used corresponding to an integrated luminosity of $138\,\text{fb}^{-1}$ of proton-proton collisions at $\sqrt{s} = 13\,\text{TeV}$, recorded at the CERN LHC in 2016–2018. Decay products of long-lived HNLs could interact with the shielding materials in the CMS muon system and create hadronic and electromagnetic showers detected in the muon chambers. This distinctive signature provides a unique handle to search for HNLs with masses below 4 GeV and proper decay lengths of the order of meters. The signature is sensitive to HNL couplings to all three generations of leptons. Candidate events are required to contain a prompt electron or muon originating from a vertex on the beam axis and a displaced shower in the muon chambers. No significant deviations from the standard model background expectation are observed. In the electron (muon) channel, the most stringent limits to date are set for HNLs in the mass range of 2.1–3.0 (1.9–3.3) GeV, reaching mixing matrix element squared values as low as $8.6\,(4.6) \times 10^{-6}$.

Submitted to Physical Review D

*See Appendix A for the list of collaboration members

Transverse asymmetry of individual γ-rays in the ^{139}La($\vec{n}$, γ)^{140}La reaction

M. Okuizumi,[1] C. J. Auton,[2,1] S. Endo,[1,3] H. Fujioka,[4] K. Hirota,[5] T. Ino,[5] K. Ishizaki,[1] A. Kimura,[3] M. Kitaguchi,[1] J. Koga,[6] S. Makise,[6] Y. Niinomi,[1] T. Oku,[3,7] T. Okudaira,[1,3] K. Sakai,[3] T. Shima,[8] H. M. Shimizu,[1] H. Tada,[1] S. Takada,[9,3] S. Takahashi,[7] Y. Tani,[4] T. Yamamoto,[1] H. Yoshikawa,[8] and T. Yoshioka[6]

[1] *Nagoya University, Furocho, Chikusa, Nagoya 464-8602, Japan*
[2] *Indiana University, Bloomington, Indiana 47401, USA*
[3] *Japan Atomic Energy Agency, 2-1 Shirane, Tokai 319-1195, Japan*
[4] *Tokyo Institute of Technology, Meguro, Tokyo 152-8551, Japan*
[5] *KEK, 1-1 Oho, Tsukuba, Ibaraki 305-0801, Japan*
[6] *Kyushu University, 744 Motooka, Nishi, Fukuoka 819-0395, Japan*
[7] *Ibaraki University, 2-1-1 Bunkyo, mito, Ibaraki 310-8512, Japan*
[8] *Osaka University, 10-1 Mihogaoka, Ibaraki, Osaka 567-0047, Japan*
[9] *Tohoku University, 2-1-1 Katahira, Aoba, Sendai, Miyagi 980-8577, Japan*

(Dated: March 1, 2024)

The enhancement of the parity-violating asymmetry in the vicinity of p-wave compound nuclear resonances was observed for a variety of medium-heavy nuclei. The enhanced parity-violating asymmetry can be understood using the s-p mixing model. The s-p mixing model predicts several neutron energy-dependent angular correlations between the neutron momentum $\vec{k}_n$, neutron spin $\vec{\sigma}_n$, γ-ray momentum $\vec{k}_\gamma$, and γ-ray polarization $\vec{\sigma}_\gamma$ in the (n,γ) reaction. In this paper, the improved value of the transverse asymmetry of γ-ray emissions, corresponding to a correlation term $\vec{\sigma}_n \cdot (\vec{k}_n \times \vec{k}_\gamma)$ in the ^{139}La$(\vec{n},\gamma)^{140}$La reaction, and the transverse asymmetries in the transitions to several low excited states of ^{140}La are reported.

Keywords: compound nuclei, partial wave interference, neutron radiative capture reaction

I. INTRODUCTION

A large parity-violating asymmetry of the cross section has been observed in a p-wave resonance of the ^{139}La + n compound state [1]. The magnitude of the parity-violating asymmetry amounts to 10^6 times larger than that of nucleon-nucleon scattering, which is dominated by the interference between parity-unfavored partial waves via the contribution of the weak interaction in the compound nuclear process [2–5]. The enhanced parity-violating asymmetry is explained as the result of the interference between the p-wave resonance and neighboring s-wave resonances (s-p mixing model) [6]. The s-p mixing model predicts angular correlations between neutron momentum, neutron spin, γ-ray momentum, and γ-ray spin depending on neutron energy in (n,γ) reactions [7]. Investigating these spin angular correlations is essential for understanding the parity violation enhancement mechanism.

Angular correlations in the (n,γ) reaction of several nuclei have been observed for the integral γ-spectrum [8]. Recently, the neutron energy dependence of the angular distribution was measured for individual γ-rays emitted from p-wave resonances in ^{139}La [9, 10], ^{117}Sn [11], and ^{132}Xe [12] using an intense pulsed neutron beam at the Material and Life Science Experimental Facility (MLF) of the Japan Proton Accelerator Research Complex (J-PARC). The transverse asymmetry was also measured in ^{139}La [13, 14] and ^{117}Sn [15]. The transverse asymmetry corresponds to the correlation term $a_2\vec{\sigma}_n \cdot (\vec{k}_n \times \vec{k}_\gamma)$ in Ref. [7], where $\vec{\sigma}_n$, $\vec{k}_n$, and $\vec{k}_\gamma$ are unit vectors for the neutron spin, neutron momentum, and γ-ray momentum direction, respectively.

We have accumulated more statistics with the setup described in Ref. [13, 14]. The transverse asymmetry was measured with improved statistics for γ-ray transition to the ground state and also low-excited states.

II. EXPERIMENT AND ANALYSIS

A. Experiment

The measurements were carried out using the Accurate Neutron-Nucleus Reaction Measurement Instrument (ANNRI) instrument on beamline-04 of MLF at J-PARC [16]. The neutron energy was determined using the neutron time-of-flight (TOF) method. The neutron beam was polarized using a ^{3}He spin-filter, which makes use of the large spin dependent cross-section of ^{3}He nuclei.

The ^{3}He spin was flipped approximately every four hours using the adiabatic fast-passage NMR method [17]. The γ-ray energy was measured with germanium detectors. Li-Glass detectors were installed downstream of the target, which are used for neutron transmission measurements.

The ANNRI instrument uses two types of Ge detectors: cluster-type and coaxial-type detectors, each positioned to surround the target in both the vertical and horizontal directions [18]. For this analysis, only the up- and down-cluster detectors were utilized. Further details on the experimental setup and measurements are described in Ref. [13].